



Zwitterionic Nanogels and Microgels: An Overview on Their Synthesis and Applications

Pabitra Saha, Ritabrata Ganguly, Xin Li, Rohan Das, Nikhil K. Singha, and Andrij Pich*

Zwitterionic polymers by virtue of their unique chemical and physical attributes have attracted researchers in recent years. The simultaneous presence of positive and negative charges in the same repeat unit renders them of various interesting properties such as superhydrophilicity, which has significantly broadened their scope for being used in different applications. Among polyzwitterions of different architectures, micro- and/or nano-gels have started receiving attention only until recently. These 3D cross-linked colloidal structures show peculiar characteristics in context to their solution properties, which are attributable either to the comonomers present or the presence of different electrolytes and biological specimens. In this review, a concise yet detailed account is provided of the different synthetic techniques and application domains of zwitterion-based micro- and/or nanogels that have been explored in recent years. Here, the focus is kept solely on the “polybetaines,” which have garnered maximum research interest and remain the extensively studied polyzwitterions in literature. While their vast application potential in the biomedical sector is being detailed here, some other areas of scope such as using them as microreactors for the synthesis of metal nanoparticles or making smart membranes for water-treatment are discussed in this minireview as well.

1. Introduction

Nanomaterials of different architectures like nanoparticles,^[1] micelles, polymersomes,^[2] and dendrimers have found biomedical usage in recent times. However, their application in this regard is somewhat limited because of a variety of factors, such as untimely drug discharge, deficient in vivo bio-distribution, lack of regio-specificity, and also high cytotoxicity.^[3–5] Compared to the other nano-sized materials, the aqueous functional nanogels or microgels (typically 0.1–100 μm in size), owing to their 3D polymeric network-like structure have drawn the attention of researchers due to their smaller size, higher surface area, and porosity.^[6–8] Not only do they exhibit high structural stability, but they are highly biocompatible as well.^[9,10] Depending on the functionalities present along with the network, the microgels respond to different external stimuli like temperature,^[11] pH,^[12] electric field,^[13] and ionic strength,^[14–18] which manifests in physical and chemical

processes such as swelling and degradation.^[19,20] In this regard, careful tuning of the type and the amount of such functional groups, along with their distribution in the 3D microgel network are crucial in the development of microgel-based materials in high-ended biomedical applications such as targeted drug delivery,^[21–23] facile bio-conjugation,^[24,25] bio-imaging,^[26] tissue regeneration, as well as catalysis,^[27] and smart surface coatings.^[28–31] Compared to hydrogels (bulk gels), not only do the microgels show biocompatibility of similar degree, owing to their smaller sizes, but they also hold significant advantages over hydrogels,^[32] especially when utilized as biomaterials: (i) microgels respond faster to the external stimuli compared to bulk hydrogels.^[33] (ii) microgels can be chemically modified such as they can circulate in the bloodstream over a longer period and in some cases, their bio-degradable nature permits them to be rapidly eliminated from the body.^[34,35] (iii) microgels can be used as building blocks in the designing of medical devices that result in a substantial improvement in their workability.^[36,37]

Of the aforementioned different types of stimuli, in the context of microgels, the effect of temperature remains to be the most-studied and well-understood.^[38–40] Some polymers, for example, display a lower critical solution temperature (LCST) behavior in the aqueous medium. Below the LCST, the polymer chains remain in the same phase as that of the solvent molecules, whereas above the LCST, an entropy-driven phase separation of the


P. Saha, X. Li, Prof. A. Pich
DWI – Leibniz-Institute for Interactive Materials
52074 Aachen, Germany
E-mail: pich@dwil.rwth-aachen.de

P. Saha, X. Li, Prof. A. Pich
Institute of Technical and Macromolecular Chemistry
RWTH Aachen University
52062 Aachen, Germany

R. Ganguly, Prof. N. K. Singha
Rubber Technology Centre
Indian Institute of Technology, Kharagpur
Kharagpur 721302, India

R. Das
Luxembourg Institute of Science and Technology (LIST)
Avenue des Hauts-Fourneaux, Esch-sur-Alzette 4362, Luxembourg

Prof. A. Pich
Aachen Maastricht Institute for Biobased Materials (AMIBM)
Maastricht University
Geleen 6167, The Netherlands

 The ORCID identification number(s) for the author(s) of this article can be found under <https://doi.org/10.1002/marc.202100112>

© 2021 The Authors. Macromolecular Rapid Communications published by Wiley-VCH GmbH. This is an open access article under the terms of the Creative Commons Attribution License, which permits use, distribution and reproduction in any medium, provided the original work is properly cited.

DOI: 10.1002/marc.202100112

polymer chains occurs from the solvent medium.^[41–44] Poly(*N*-vinylcaprolactam) (PVCL) and poly(*N*-isopropylacrylamide) (PNIPAM) are the two most extensively studied polymers exhibiting LCST-behavior and both of them have been used to fabricate microgels of different types of applications.^[45–47] The LCSTs of such microgels can be tuned to higher values via the incorporation of hydrophilic functional groups. Apart from temperature, microgels responsive to other external stimuli such as pH,^[48] ionic strength,^[49] and light^[50–52] can be synthesized, depending on the type of functional comonomers chosen. Also, from literature, it is often observed that functional groups responsive to different stimuli can be loaded in the same microgel system, which works synergistically to broaden the scope for the potential applications of these microgels.^[53–55]

A classic example of such a hydrophilic functional molecule is a zwitterion. Zwitterions are found in our body in the form of essential amino acids like alanine, valine, phenylalanine, taurine, and so on.^[56–59] Depending on the pH of the solution, they are present as either positively charged or negatively charged species and the pH at which they are electrically neutral is called their isoelectric point.^[60,61] Zwitterionic polymers can be synthesized containing a stoichiometric equivalence of positively (quaternized nitrogen atom) and negatively (sulfonate, carboxylate, phosphate)-charged groups present along the main polymer backbone. Based on the negatively charged groups, the synthetic polyzwitterions or polybetaines can be classified mainly into three types, i.e., poly(sulfobetaine) (PSB), poly(carboxybetaine) (PCB), and poly(2-methacryloyloxyethyl phosphorylcholine) (PMPC).^[62–64] Polyzwitterions are a special type of polyampholytes. While in polyampholytes, the positively and negatively charged groups are highly dependent on the pH of the medium,^[65–67] in polybetaines or polyzwitterions, the charged groups maintain their charge neutrality over a range of pH due to the high density of opposite ion-pairs bound to the polymer backbone. The synthesis of polyampholyte microgels and their applications in different domains are also well-documented in literature.^[68–70] Though both positive and negative charges are present in polyampholyte microgels, there is no defined order in which these charges might be distributed respectively to one another over the entire microgel network.^[71] Unlike in polybetaines, the two types of charges can be present in stoichiometric nonequivalence, thereby making the overall charge weighted toward being either positive or negative (polyanionic or polycationic microgels).^[72–76] Therefore, unlike polyampholytes, zwitterionic microgels exhibit some special characteristic features. Due to the prevalence of strong coulombic interactions along the polymer backbone, the zwitterionic microgels become superhydrophilic and as a result, they do not behave as typical polyelectrolytes and show great tolerance to extremely saline condition.^[77] Polyzwitterions have been assessed to be fascinating compounds for the last few decades and due to the structural similarities to the phospholipid, a major component of cell membranes, they are recognized as highly biocompatible.^[78,79] With this in mind, much attention has been given to the zwitterionic micro-and/or nanogel toward the mimicking of biological cell membranes by tailoring the surface of the polymers as they offer excellent resistance to bio-fouling against various foulant materials.^[80,81] As a consequence of that, they can be prevalently considered as attractive candidates in the making of

biomedical devices.^[82–84] Interestingly, polyzwitterions are also thermo-responsive as they exhibit an upper critical solution temperature (UCST), below which the zwitterionic polymer chains are in collapsed state, due to the high coulombic attraction force between two opposite ion-pairs. Above UCST, the thermal energy disrupts ionic interactions between the zwitterions and they form hydrogen bonds with water molecules, inducing the solvation of polymer chains.^[85–89] Moreover, their sensitivity to reversible changes in the presence of temperature can also be exploited to design stimuli-responsive zwitterionic microgels for various applications.

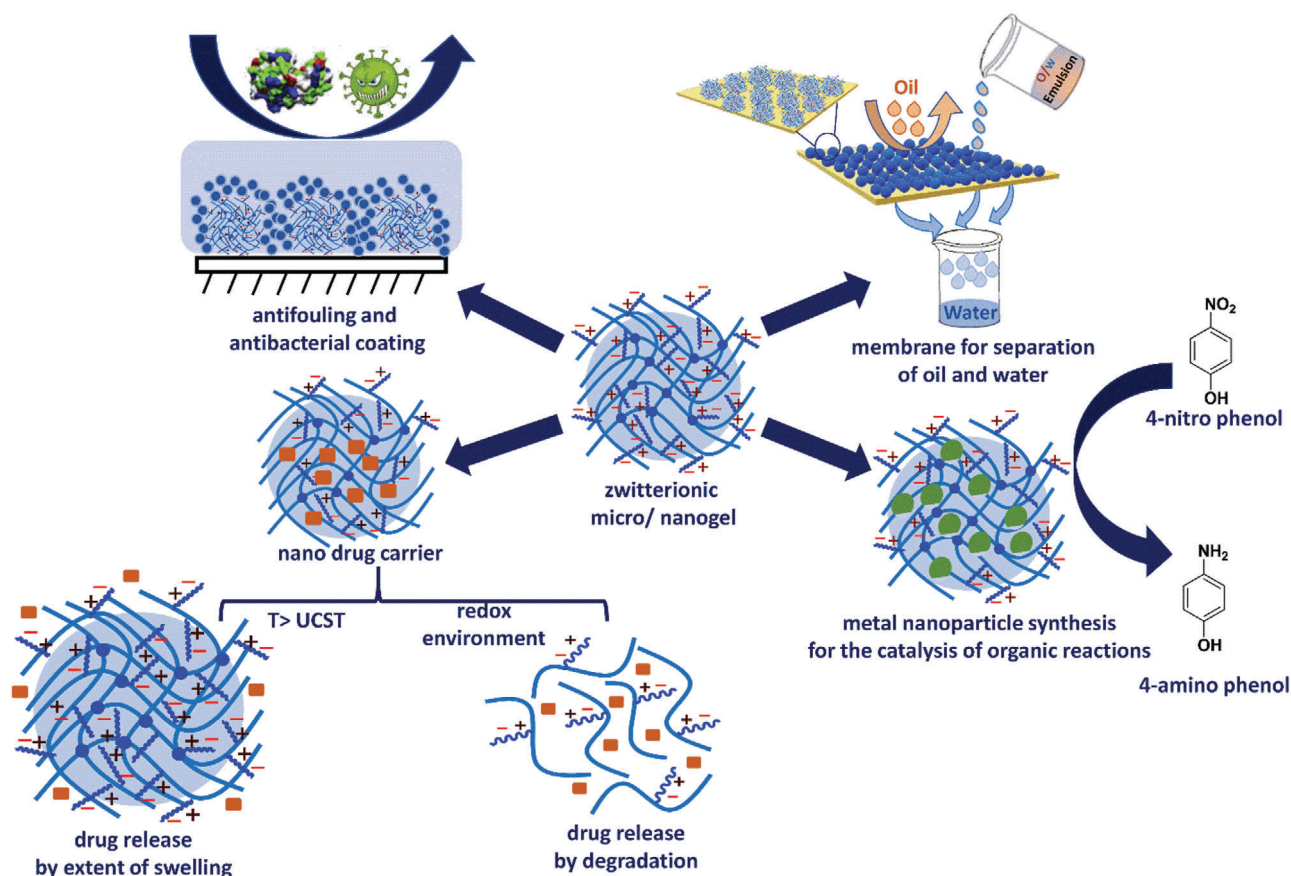
Though the basic synthetic procedures and structure–property relationship of different zwitterionic architectural polymers have been extensively reviewed in some articles, yet such high-quality articles are very few. The majority of these articles focuses on the specific aspects like membrane-applications of polyzwitterions,^[90] or their stimuli-responsive behaviors,^[91,92] however, illustrating mainly zwitterionic linear polymer, block or graft copolymer, and hydrogels.^[93,94] In summary, the synthesis and application of zwitterionic (especially betaine) micro-and/or nanogels have hardly been reviewed systematically, like we have tried here in this minireview (see **Scheme 1**). This present review could not be comprehensive; decisions had to be made to keep the contents reasonable, which inevitably may have made it descriptive to a certain extent. A thin borderline exists between the terms nanogel and microgel as they are relative to each other and henceforth, they will be termed as nanogels or sometimes microgels as per the nomenclature given by the respective group of authors.

2. Synthesis of Zwitterionic Nanogels and Microgels

Unlike the synthesis of polyampholyte microgels where simultaneous incorporation of both positively charged and negatively charged monomers makes it difficult to regulate the solution pH during the synthesis steps,^[95] for zwitterionic microgels, regulating the pH is relatively simpler. Zwitterions contain an equal number of positive and negative charges inside the same molecule, which renders them to be electrically neutral. Thus, the synthetic steps involving polyzwitterions are largely pH-independent. Although there have been significant challenges in the last few decades regarding the synthesis of zwitterionic microgels, mainly because of their high hydrophilicity and high solvent selectivity, in recent times, researchers have successfully come up with a variety of novel synthetic routes to prepare zwitterionic micro-and/or nanogels.

2.1. Post-Modification

This technique is rarely reported in literature. Generally, a pre-synthesized functional microgel is used as a precursor and its functionality can be utilized to convert it to a zwitterionic group by post-modification under particular reaction conditions.^[96,97] Recently, Sahiner and co-workers have reported the synthesis of zwitterionic microgels by the betanization of poly(ethylene imine) (PEI) microgels.^[98] First, the PEI microgels were synthesized from the branched PEI polymer (molecular



Scheme 1. Schematic representation of applications of zwitterionic micro/nanogels.

weight $\approx 1800 \text{ g mol}^{-1}$) by cross-linking with divinyl sulfone (DVS) cross-linker in the presence of bis(2-ethylhexyl) sulfosuccinate sodium salt (AOT) surfactant in a water-in-gasoline micro-emulsion technique. Finally, the PEI microgels were betanized by reacting with 1,3-propane sultone (1:1 molar ratio) in deionized water and purified by dialysis (see **Figure 1a**). They observed that the betanized PEI (b-PEI) zwitterionic microgels became biocompatible and anti-bacterial, and the betanization upon PEI microgels increased the different dye adsorption (such as methylene blue, MB) capabilities of the resultant zwitterionic microgels as well (see **Figure 1b**).

Though, technically not a post-modification approach, Sinclair and co-workers proposed an interesting top-down method of obtaining microgels from previously existing bulk precursors. Here, carboxybetaine-based bulk gels were broken down mechanically into particles in dimensions of 15–30 μm , which are significantly larger than microgels synthesized via traditional means. This “intermediate” size enables them to retain properties associated with both micro and macro dimensions; for example, strength and elasticity atypical to bulk gels on one hand and high surface area on the other.^[99]

2.2. Aqueous Precipitation Polymerization

Generally, in this polymerization technique, a water-soluble thermo-responsive monomer is introduced simultaneously

along with a water-soluble initiator, a cross-linker, and surfactants (optional) in a reaction chamber, and the polymerization temperature is set depending on the volume phase transition temperature of the corresponding polymer. For example, thermo-responsive PVCL and PNIPAM microgels are synthesized in water at $\approx 70 \text{ }^\circ\text{C}$ (above its LCST $\approx 32 \text{ }^\circ\text{C}$), using *N,N'*-methylenebis(acrylamides) (BIS) cross-linker. Initially, the oligomeric chains start to grow until a critical chain length is reached. Post that, the chains collapse to form microgel nuclei or precursors. Following that, over time they start aggregating to form microgels.^[100,101] Das and co-workers first adapted the free-radical precipitation polymerization method to synthesize poly(*N*-isopropylacrylamide-sulfobetaine) (PNIPAM-PSB) zwitterionic microgel via a surfactant-free process in the water medium. The polymerization temperature was maintained at $70 \text{ }^\circ\text{C}$ and PNIPAM and zwitterionic sulfobetaine segments got incorporated randomly with respect to one another.^[102] The presence of BIS resulted in the formation of a cross-linked network structure. Owing to their LCST-inducing nature, the PNIPAM segments collapsed related to their phase separation from the aqueous medium, which ultimately leads to the microgels precipitating out. The solution properties and size studies of the microgel particles proved that the incorporation of the superhydrophilic zwitterionic segment increased the LCST of the PNIPAM-based zwitterionic (PNIPAM-PSB) microgels and the size of the microgels lied in a range of 650–1200 nm. It was

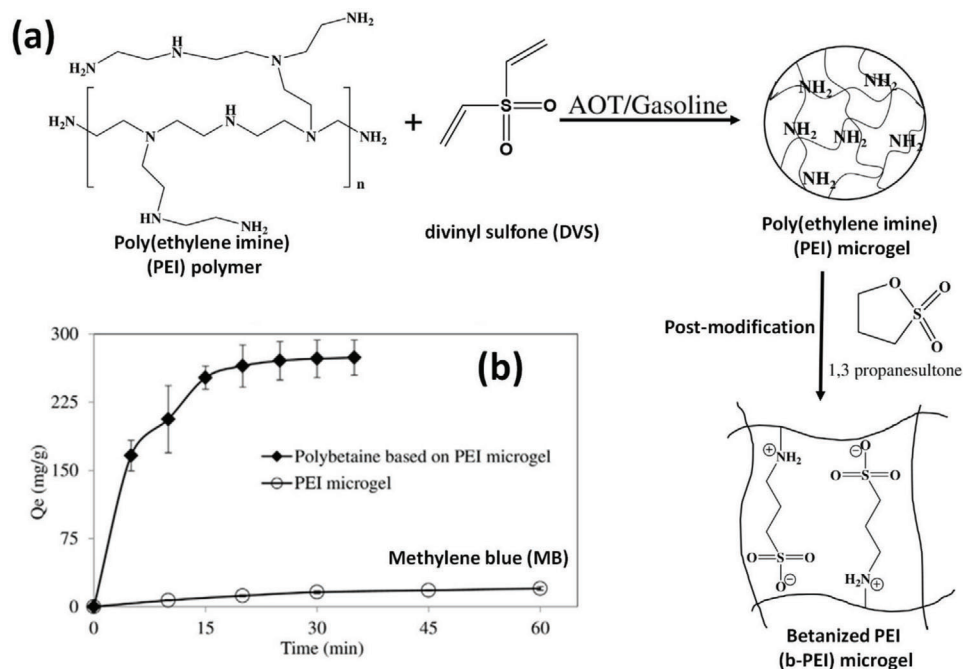


Figure 1. a) Synthesis of zwitterionic microgel by betanization with PEI microgel and b) methylene blue (MB) dye adsorption profile of unmodified and modified PEI microgels. Reproduced with permission.^[98] Copyright 2017, Elsevier.

observed that a higher amount of sulfobetaine effectively increased the size, as well as the LCST of the microgels due to its increased hydrophilicity (**Figure 2b**). However, despite the presence of the zwitterionic sulfobetaine segments, the microgels did not exhibit any anti-polyelectrolyte effect in the presence of different salts of the Hoffmeister series. The authors have attributed this to the relatively lower incorporation and uncontrolled distribution of the zwitterionic groups in the microgels.^[103,104] Subsequently, Schmid and co-workers synthesized zwitterionic PNIPAM-PSB and poly(*N*-vinylcaprolactam-sulfobetaine) (PVCL-PSB) microgels in a precipitation polymerization technique and in the presence of sodium dodecyl sulfonate (SDS) surfactant. The microgels thus formed were much smaller (140–200 nm) than was observed when no surfactants were used due to electrostatic repulsive interaction between the surfactant molecules (see **Figure 2c**).^[105]

Sometimes, the use of a single stimulus (e.g., only temperature) working at a different range is advantageous over multiple stimuli (e.g., both temperature and pH) in the formulation of smart materials to avoid the complexity in terms of understanding their workability in various applications.^[106,107] Taking that into account, Arotcaréna and co-workers have synthesized zwitterionic PNIPAM-PSB block copolymers by RAFT polymerization with different block lengths of both constituents and they studied the reversible switching (“inside–outside”) of the polymer colloid aggregates controlled by the simple thermal stimulus at a wide range of temperature.^[108] Nonetheless, the zwitterionic core-shell nanogels exhibiting both UCST-LCST transition were first communicated by Rajan and co-workers where they could tune the dual transition temperatures by varying the concentration of the zwitterionic microgel solution (see **Figure 3a,b**).^[109] However, they did not propose any mechanism behind this

macro-RAFT mediated microgel synthesis in their report. Inspired by their findings, our group has recently reported a detailed study of thermo-responsive zwitterionic poly(sulfobetaine) (PSB)-based PVCL microgels (see **Figure 3c**) with a plausible mechanism of microgel formation at different stages of the reaction. Here, we adapted a surfactant-free RAFT precipitation polymerization to synthesize the zwitterionic microgels and it has been observed that the LCST of the PSB-PVCL microgels varied with the amount of PSB macro-RAFT and the molecular chain length as well.^[110] We found that not only the amount of the different molecular weight PSB macro-RAFT shows a strong effect on their respective UV–vis cloud points, but also the amount of the BIS cross-linker used during the microgel synthesis could regulate the LCST of the zwitterionic microgels (see **Figure 3d,e**).

Zwitterionic microgels can also be prepared singularly (without using any LCST-type polymers) by copolymerizing zwitterionic monomer with different cross-linkers in an aqueous precipitation polymerization in the absence of surfactants. Generally, most of the poly(sulfobetaine) (PSB) zwitterionic polymers have proved to show the UCST much lower than the physiological temperature because of the weakening of the strong intramolecular interaction between the opposite charges (see **Figure 3b**), leading to the formation of hydrogen bonding between the ions and the water molecules.^[111] Therefore, this kind of sulfobetaine-based zwitterionic polymers suffers their usability as a thermo-responsive drug delivery system in hyperthermia cancer therapy.^[112] With this in mind, Peng and co-workers introduced a hydrophobic benzsulfamide group as an anionic segment into the zwitterionic structure that significantly uplifted the UCST of the corresponding sulfamide-based poly(2-(2-(methacryloyloxy)ethyl)dimethylammonio)acetyl

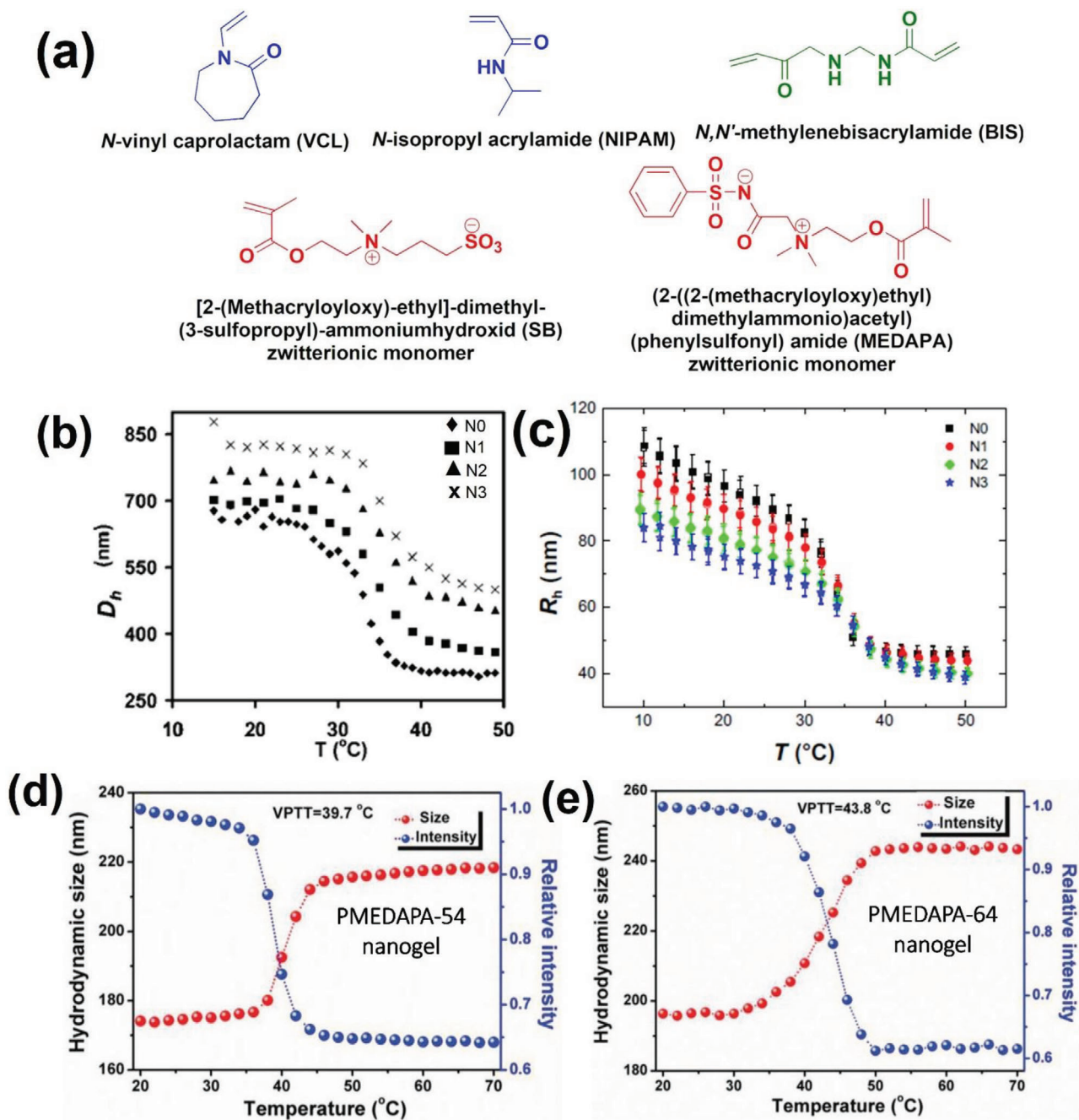


Figure 2. a) (From left to right) Chemical structures of VCL monomer, NIPAM monomer, BIS cross-linker, SB zwitterionic monomer, and MEDAPA zwitterionic monomer, and change in particle size/radius of different sulfobetaine loaded zwitterionic (PNIPAM-PSB) microgels b) in absence of surfactant. Reproduced with permission.^[102] Copyright 2008, American Chemical Society. and c) in the presence of sodium dodecyl sulfate (SDS) surfactant; where N0, N1, N2, and N3 are the microgels prepared with 0, 2, 4, and 6 mol% of SB monomer. Reproduced with permission.^[105] Copyright 2015, Springer, respectively. Change in UCST-type VPTT of PMEDAPA nanogels d) PMEDAPA-54 and e) PMEDAPA-64; where PMEDAPA-54 and 64 stand for PMEDAPA nanogels prepared with 54 and 64 molar ratios of cross-linker, respectively. Reproduced with permission.^[113] Copyright 2017, John Wiley & Sons.

phenylsulfonyl) amide (PMEDAPA) zwitterionic nanogels close to the physiological temperature (see the chemical structure of MEDAPA monomer, Figure 2a). They adapted an aqueous precipitation polymerization technique to prepare these nanogels by using ethyleneglycol dimethacrylate (EGDMA) and bis(acryloyl)cystamine (BAC) as cross-linkers with various cross-

linking degrees to regulate the UCST-type volume phase transition temperature (VPTT) of the nanogels by switching between collapsed and swollen state. The higher the cross-linker molar ratio used, the higher is the VPTT of the nanogels due to their more compact network structures (see Figure 2d,e).^[113] Moreover, the PMEDAPA nanogels showed excellent biocompatibility

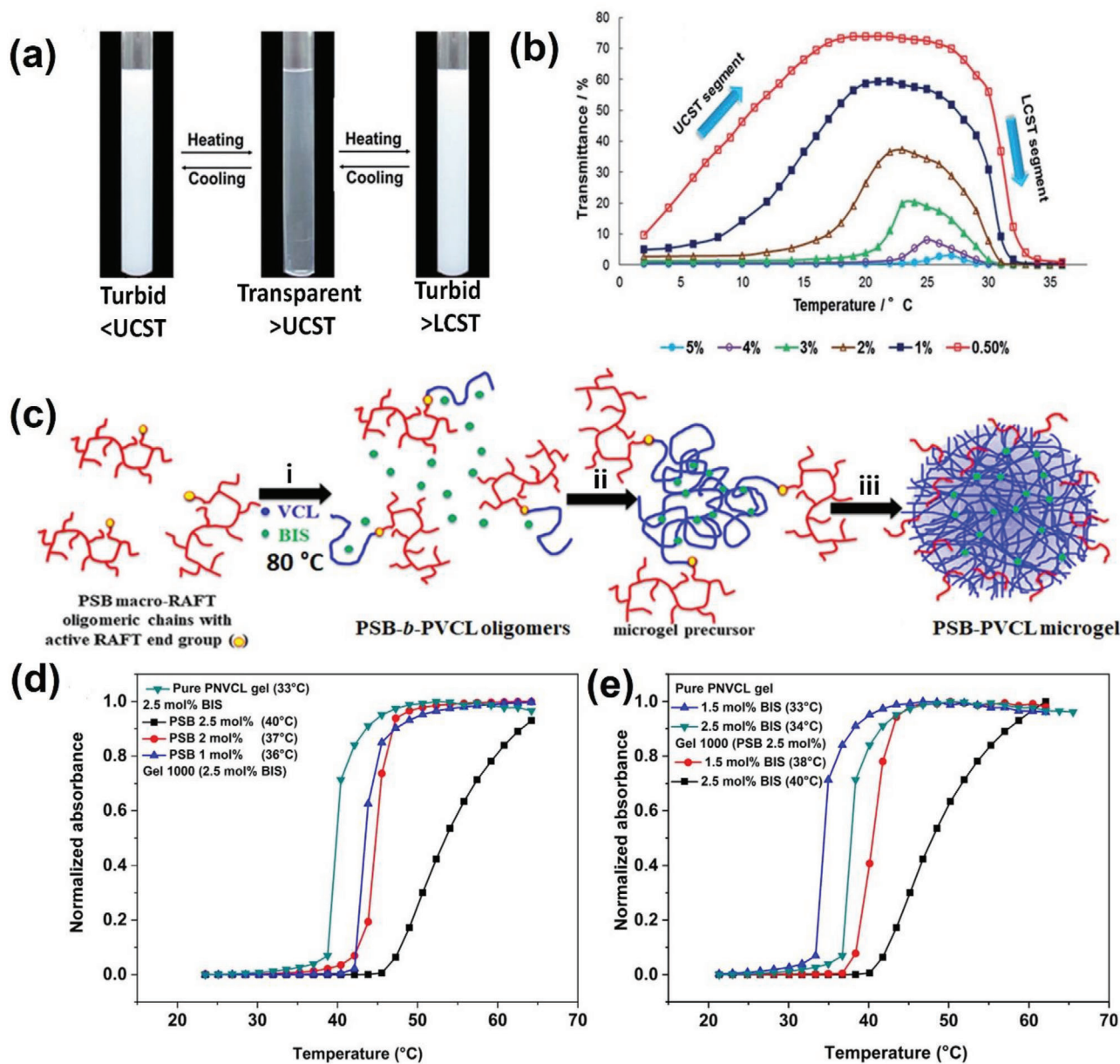


Figure 3. a) Photographs of dual thermo-responsive zwitterionic microgel, showing both UCST and LCST, and b) their UV-vis cloud points at different microgel concentrations. Reproduced with permission.^[109] Copyright 2017, John Wiley & Sons. c) Schematic diagram of precipitation polymerization to produce thermo-responsive zwitterionic microgel; i) formation of oligomer radicals, ii) microgel nucleation, iii) precipitation of microgels, cloud points of zwitterionic microgels (Gel 1000) prepared with PSB 1000 zwitterionic macro-RAFT with d) different PSB content (1, 2, and 2.5 mol%), and e) different BIS cross-linker content (1.5 and 2.5 mol%). Reproduced with permission.^[110] Copyright 2019, Elsevier.

and prolonged blood circulation similar to the other synthetic polyzwitterions and thus, they were used as microwave-triggered on-demand drug vectors for enhanced cancer therapy. Later on, He and co-workers have developed zwitterionic poly(*N*-isopropylacrylamide-*co*-acrylic acid-*co*-1-propyl-3-vinylimidazole sulfonate) (P(NIPAM-*co*-AA-*co*-PVIS)) microgels using PVIS as a zwitterionic monomer in a purely water-based surfactant-free precipitation polymerization. They used this microgel model to highly resist the nonspecific protein adhesion on their surfaces, and more importantly fabricate a novel electro-

chemical immunosensor to detect an aminoglycoside antibiotic, streptomycin (STR) from milk.^[114]

2.3. Nonaqueous Precipitation Polymerization

Nonaqueous precipitation polymerization is often termed dispersion polymerization in which the monomers, initiator, and stabilizer are dissolved together in a particular solvent or in a mixture of solvents to form a homogeneous mixture.^[115] Once

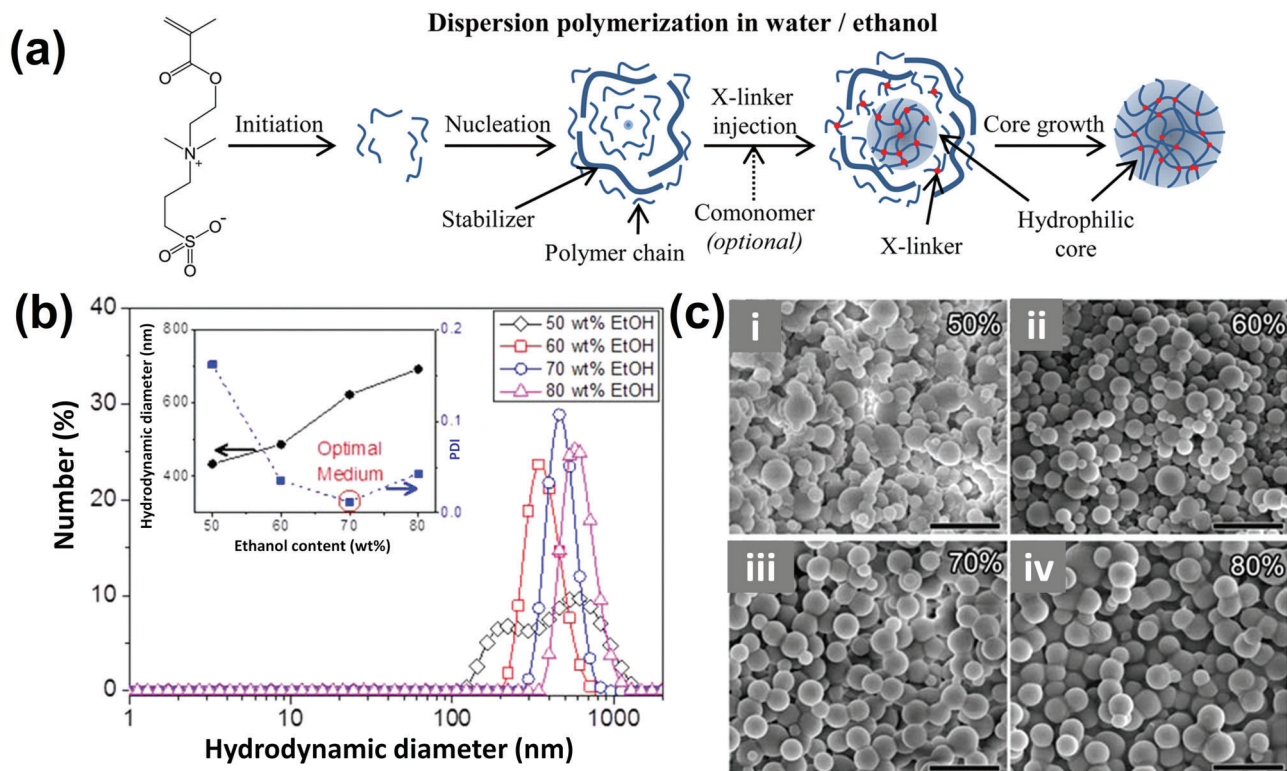


Figure 4. a) Schematic presentation of dispersion polymerization using water/ethanol mixture of solvents, b) Particle distribution index and c) SEM images of the zwitterionic microgels with the variation in water:ethanol volume ratio (scale bar 2 μm). Reproduced with permission.^[119] Copyright 2016, American Chemical Society.

the critical chain length is reached, the initially unstable polymer chains start coagulating with others until a stable polymer dispersion is formed.^[116,117] The stabilizer or dispersant molecules (typically block or graft copolymers) present in the solution attach covalently to the surface of the growing particles and prevent the particle coagulation, thereby imparting colloidal stability to the system (see **Figure 4a**). This technique allows the incorporation of various comonomers at particular stages of polymerization that improve the functionality of the polymer particles. This is a simple and direct approach used to produce mainly hydrophobic or amphiphilic microgels. However, the synthesis of hydrophilic zwitterionic microgels via dispersion polymerization is also explored in literature. The obvious challenge is the high affinity of the growing polyzwitterionic chains toward the water, which greatly prohibits the formation of the microgel nuclei or precursor particles.^[118] Varnoo-faderani and co-workers circumvented this limitation to synthesize functional zwitterionic microgels by optimizing the typical binary solvent ratio and by controlling the composition of the reaction mixture at various stages of polymerization.^[119] In a typical synthesis, sulfobetaine (SB) monomer, ammonium persulfate (APS) initiator, and poly(vinylpyrrolidone) (PVP) stabilizer were allowed to react in a water/ethanol solvent mixture at 50 °C. The different volume ratio between water and ethanol was also optimized to obtain the zwitterionic microgels with smaller size and low particle distribution index, PDI (see **Figure 4b**). After 30 min of the reaction ($\approx 5\%$ conversion), different types and amounts of cross-linkers were introduced into the

solution mixture to produce the functional zwitterionic microgels. Scanning electron microscopic (SEM) images showed that an increase in the ethanol content ($>80\%$) resulted in larger particle size and particle agglomeration due to the insufficient steric stabilization by APS initiator, and undergoing faster reaction (see **Figure 4c**). Different types of comonomers such as 2-ethylhexyl methacrylate (2-EHMA), butyl acrylate (BuA), methyl methacrylate (MMA), hydroxyethyl methacrylate (HEMA), acrylamide (AAm), and dopamine methacrylamide (Dopa-MA) were used in this study to obtain monodisperse well-defined versatile functional zwitterionic microgels. The widely different types of comonomers used here, ranging from hydrophobic to hydrophilic in a single microgel particle expanded the application potential of these zwitterionic microgels.

Because of the washing-off of the zwitterionic polymers from the hydrophobic surfaces due to their poor miscibility, recently, Huang and co-workers designed the semi-interpenetrating polymer networked (SIPN) zwitterionic microgels composed of PSB zwitterionic polymers and hydrophobic poly(ether sulfone) (PES) matrix in a one-pot dispersion polymerization technique.^[120] First, a PSB/PES microgel was synthesized at 100 °C for 24 h in the presence of AIBN thermal initiator and BIS cross-linker in dimethyl sulfoxide (DMSO) solvent and then the resulting microgel dispersion was blended with freshly prepared PES polymer matrix to prepare the casting solution (see **Figure 5a**). The rough surface of the pristine PES membrane surface (AB-0) with a lot of interconnected voids (see **Figure 5b**) became less visible when steady incorporation of PSB/PES zwitterionic microgels occurred

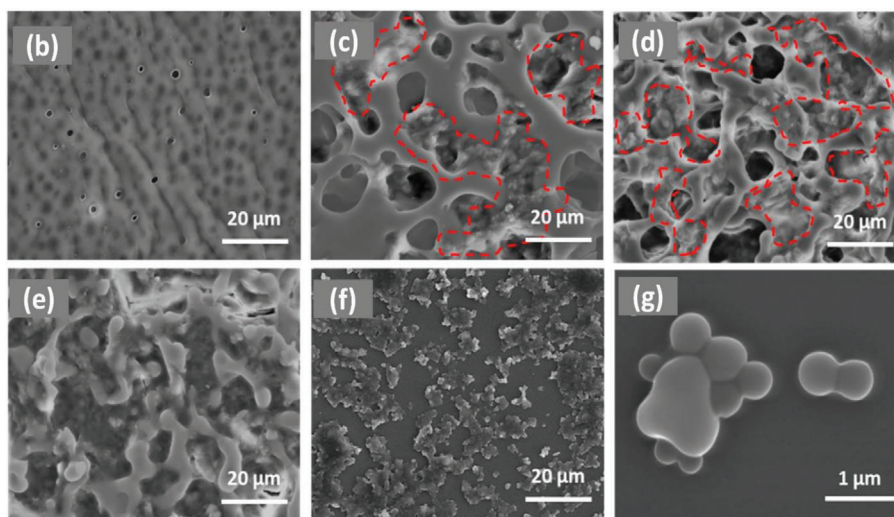
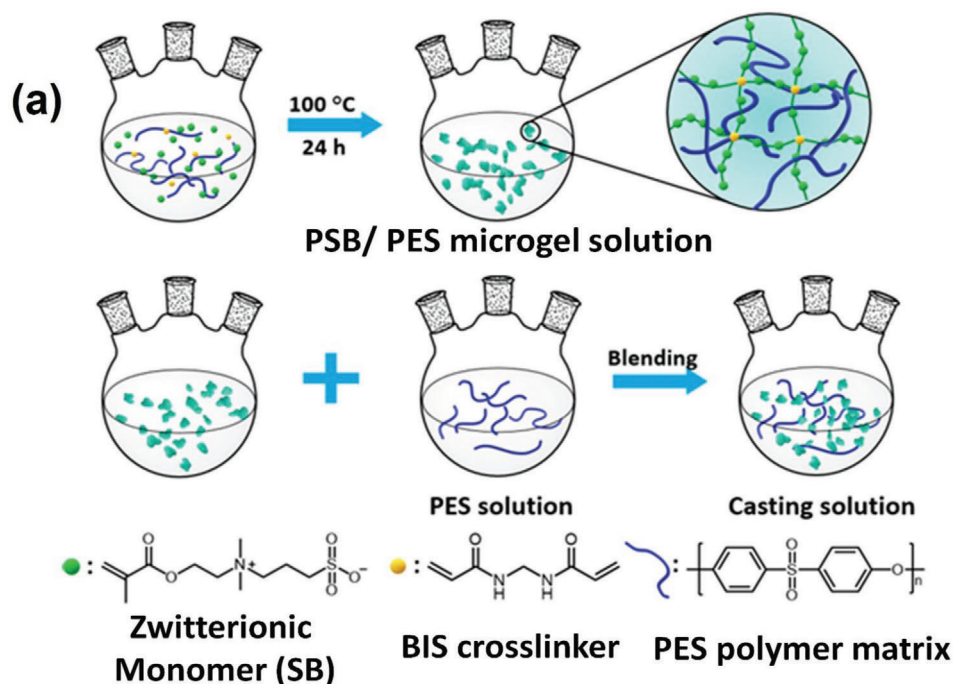


Figure 5. a) Synthesis route of the PSB/PES microgels and the preparation of the casting solutions, and SEM images of the b) AB-0 surface and c–e) zwitterionic microgel modified AB-47, AB-64, and AB-78 surfaces (scale bar 20 μm), where AB-0, AB-47, AB-64, and AB-78 denote the weight ratio (in %) of the zwitterionic PSB/PES microgel in the surface. The zwitterionic microgels were marked by red circles. f,g) Zwitterionic microgels cast from PSBMA/PES solution without blending of PES solution (scale bar 20 and 1 μm, respectively). Reproduced with permission.^[120] Copyright 2020, American Chemical Society.

by the casting with additional PES matrices (see Figure 5c,d,e). The zwitterionic microgel gradually filled the void spaces of the membrane surfaces (AB-47, AB-64, and AB-78), thus enhancing the hydrophilicity of the surface. Subsequently, the extensive entanglement of the PSB/PES zwitterionic microgels with the additional PES matrix circumvented the early washing-off of the microgel from the surface under challenging operational conditions. Figure 5f,g indicate the morphology of the surface directly cast from PSB/PES zwitterionic microgel without the addition of the PES matrix. Due to the inhomogeneity of the PSB and PES constituents, the microgels agglomerated with each other, sug-

gesting the blending process with an additional PES matrix is necessary for the mechanical endurance of the membranes. Finally, it was utilized to facilitate coat on glass slides to observe their anti-bacterial behavior using Gram-positive *Staphylococcus aureus* and Gram-negative *Escherichia coli* model bacteria.

Due to the simple and easy purification steps, the micro- and/or nanogels formed by dispersion polymerization can be preferably used for biomedical applications. Taking this advantage, Wang and co-workers first developed a variety of functional nanogels with well-defined shapes and narrow particle distribution based on this polymerization system.^[121] Nonaqueous

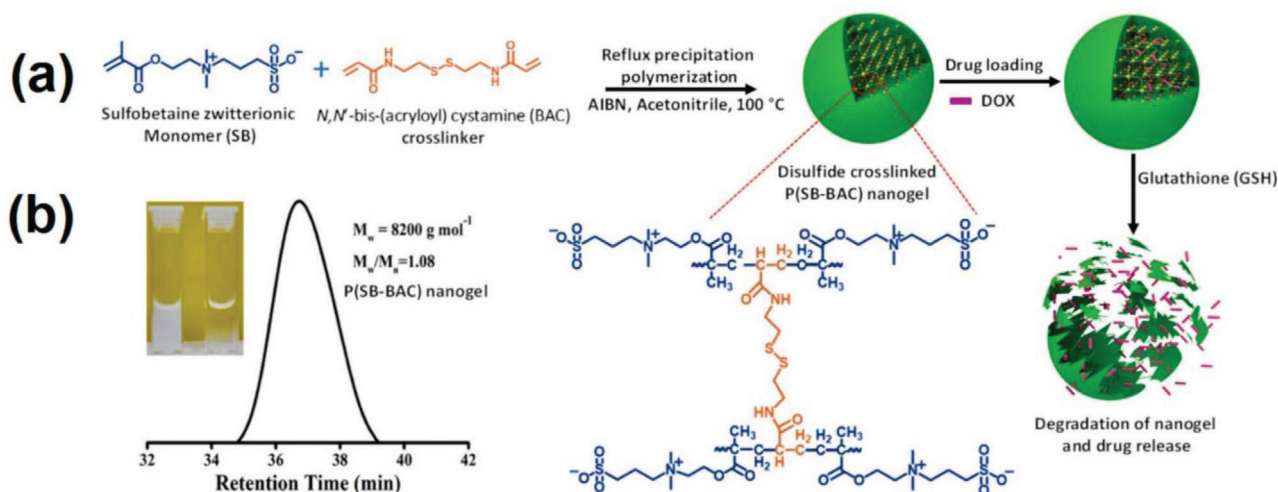


Figure 6. a) Schematic presentation of disulfide cross-linked P(SB-BAC) zwitterionic nanogel synthesis by reflux precipitation polymerization and subsequent drug loading and release, and b) GPC trace and photograph of the polymer product after nanogel degradation. Reproduced with permission.^[123] Copyright 2020, Royal Society of Chemistry.

precipitation (also called dispersion) polymerization is advantageous over conventional aqueous precipitation polymerization in terms of synthesizing highly hydrophilic acrylate-based micro- and/or nanogels solely in an organic solvent (non-aqueous medium) and due to the simple and handy reaction set up, it is also possible to produce the micro- and/or nanogels in a large scale.^[122] Men and co-workers also adapted this polymerization technique for the synthesis of biodegradable redox-responsive zwitterionic nanogels. In an exemplary synthesis, sulfbetaine (SB) monomer, disulfide type *N,N'*-bis-(acryloyl) cystamine (BAC) cross-linker were taken at different ratios in acetonitrile solvent along with 2,2'-azobisisobutyronitrile (AIBN) initiator, and the reaction mixture was immersed in an oil bath at 100 °C and for 1 h under nitrogen atmosphere. Finally, the P(SB-BAC) nanogels were spun down under centrifugation and washed three times with deionized water before lyophilization (see Figure 6a).^[123] The gel permeation chromatography (see Figure 6b) and a “turbid to transparent” transition (see the photograph, inset of Figure 6b) of the degraded polymer product with narrow dispersity indicates the nanogel degradation under reductive (GSH) environment. Furthermore, in the work of Peng and co-workers, the nonaqueous precipitation polymerization was also employed to fabricate zwitterionic poly(2-methacryloyloxyethyl phosphorylcholine) (PMPC) nanogel with *N*-vinylimidazole (VIm) content and cross-linked by disulfide bond containing cleavable BAC cross-linker. The presence of VIm moiety aided the charge conversion from a zwitterionic to a positively charged state in the nanogel at low pH 6.5, which facilitates the enhanced cellular uptake of adenocarcinomic human alveolar basal epithelial (A549) tumor cells.^[124] Along with the benefit of the PMPC zwitterionic group, serving the antifouling and long blood circulation properties, the reductive degradation of the as-prepared nanogels makes them a smart nanocarrier for targeted drug delivery. Similarly, Tian and co-workers exploited this polymerization technique to synthesize poly(phosphobetaine)-based zwitterionic nanogels, using redox-labile (both H_2O_2 and GSH) diselenide type *N,N'*-bis(methacryloyl)selenocystamine (BMASC) cross-linker.^[125]

2.4. Polymerization in Emulsion Droplets

Inverse mini-emulsions (water-in-oil, w/o) can be produced by the sonication of an aqueous dispersion of monomer, stabilizer, co-stabilizer (optional), and cross-linker (optional) in a continuous nonpolar oil phase.^[126] The mini-emulsion generally gets stability with the use of both surfactant and osmotic pressure agent, also termed as lyophobic that is completely insoluble in the continuous oil phase and prevents the particle coalescence from Ostwald ripening.^[127] Usually, the polymerization of the monomer droplet nuclei proceeds by using both oil and water-soluble initiators and the rate of the mini-emulsion polymerization strongly depends on the initiator concentration. Also, the use of a higher amount of surfactants results in more reaction loci, which also accelerates the faster rate of polymerization and high monomer to polymer conversion.^[128,129] This kind of polymerization is quite useful to synthesize copolymers having structural dissimilarities.^[130] Cheng and co-workers were the first groups to produce poly(carboxybetaine) (PCB) zwitterionic nanogels in a w/o inverse mini-emulsion polymerization. In a typical synthesis, they used CB monomer, BIS cross-linker in an aqueous phase and added this mixture into an oil phase (hexane), containing an oil-soluble thermal initiator (V-70), and sorbitan oleate (Span 80) and poly(oxyethylene-sorbitan-monooleate) (Tween 80) surfactants under vigorous shaking and sonication for 2 min. Finally, the reaction was put in an oil bath at 40 °C for 4 h with continuous nitrogen purging. The synthesized PCB nanogels were purified by centrifugation with tetrahydrofuran (THF) solvent and then washed with water several times (see Figure 7a). A significant variation in the PCB nanogel size was finely tuned by using different amounts of BIS cross-linker and by adjusting the ratio between the two surfactants as well. The nanogels were ultra-stable over a while against bovine serum protein solution at 37 °C (see Figure 7b) and they were utilized as potential drug vectors for controlled release of fluorescein isothiocyanate-tagged dextran (FITC-dextran) drug.^[131] Later on, Ajmal and co-workers re-designed this method to synthesize

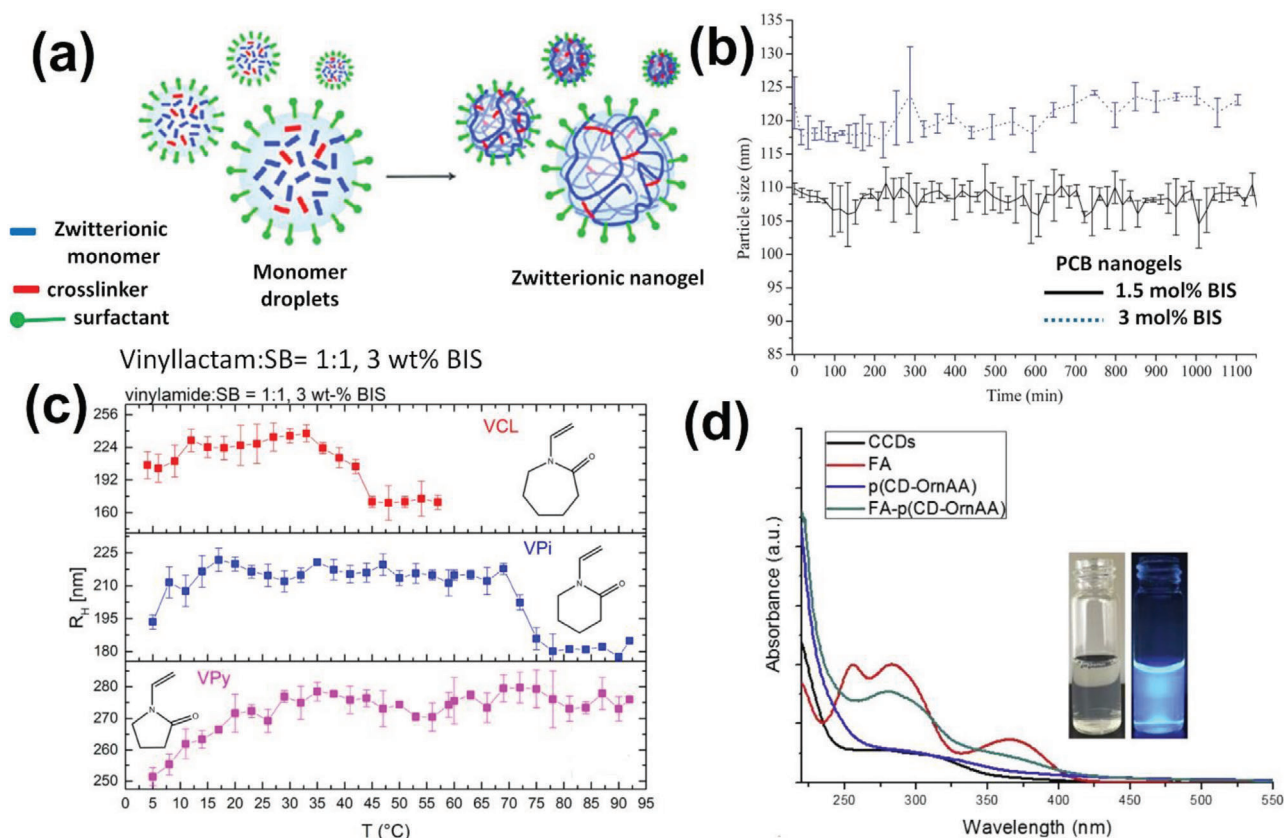


Figure 7. a) Schematic presentation of zwitterionic nanogel synthesis by mini-emulsion polymerization. Reproduced with permission.^[126] Copyright 2016, Royal Society of Chemistry. b) Stability of PCB nanogels overtime at 37 °C in the presence of bovine serum protein solution (at 1.5 mol% and 3 mol% BIS). Reproduced with permission.^[131] Copyright 2010, American Chemical Society, c) Plot of hydrodynamic radius as a function of the temperature of different poly(*N*-vinylactam-SB) microgels prepared at 3 wt% BIS concentration, showing UCST-LCST transitions, Reproduced with permission.^[133] Copyright 2018, American Chemical Society, d) Photoluminescence intensity variation with change in fluorescent CD cross-linker in P(OrnAA -CD) nanogels. Reproduced with permission.^[137] Copyright 2016, Elsevier.

zwitterionic poly(sulfobetaine) (PSB) microgels, using a water-soluble initiator, ammonium persulfate (APS) along with an accelerator *N,N,N',N'*-tetramethylethylenediamine (TEMED) at room temperature and they also showed that the PSB zwitterionic microgels thus formed acted as a nanoreaction chamber to produce Nickel (Ni) nanoparticles.^[132] Recently in our group, Pich and co-workers have reported the synthesis of doubly thermo-responsive PSB zwitterionic microgels by copolymerizing sulfobetaine (SB) with different *N*-vinylactams (*N*-vinyl caprolactam (VCL) and analogous series like *N*-vinylpiperidone (VPI), and *N*-vinylpyrrolidone (VPy)). The microgels contained a high amount of zwitterionic SB units (≈ 30 mol%) and thereby exhibiting reversible dynamic (opposite charge interaction of zwitterionic SB group) cross-linking and covalent (generated by BIS cross-linker) cross-linking. While above the UCST (≈ 12 °C), the microgels showed a temperature-triggered 'deswelling-swelling' behavior due to the disruption of ionic cross-links present in the zwitterionic SB units; an exact reverse phenomenon (swelling-deswelling) was observed at above LCST due to the breakage of the hydrogen bonds with water and enhancement of hydrophobic interaction of different lactam ring-sized poly(*N*-vinylactam) polymer chains (see Figure 7c).^[133]

Micro- and/or nanogels are well-known for their excellent drug loading-release capacity and the insertion of a fluorescent molecule into microgels provides a platform for simultaneous bio-imaging of the drug and the microgels during the delivery process.^[134–136] Considering that, Li and co-workers have developed a novel ultra-low fouling zwitterionic nanogel by copolymerizing an amino acid-based ornithine methacrylamide (OrnAA) zwitterionic monomer and fluorescent cross-linkable carbon dot (CD) cross-linker in a water-in-hexane (w/o) inverse mini-emulsion polymerization. The conjugation of folic acid (FA) as a ligand with the p(CD-OrnAA) nanogels helped the novel FA-p(CD-OrnAA) nanocarrier system for the specific internalization of the cancer cell. The characteristic UV-vis absorbance peak of CD cross-linker appearing at 270–350 nm is considered under the broad shoulder of p(CD-OrnAA) nanogel UV-vis spectrum (see Figure 7d). The incorporation of FA was found when the characteristic signal of FA appeared at 283 nm in the FA-p(CD-OrnAA) spectrum, indicating the successful fabrication of the nanogels. Moreover, the presence of CD cross-linker was also witnessed when the aqueous solution of the FA-p(CD-OrnAA) nanogel was irradiated by the UV light of 350 nm wavelength resulting in a strong blue emission (see inset of Figure 7d). Later on, they

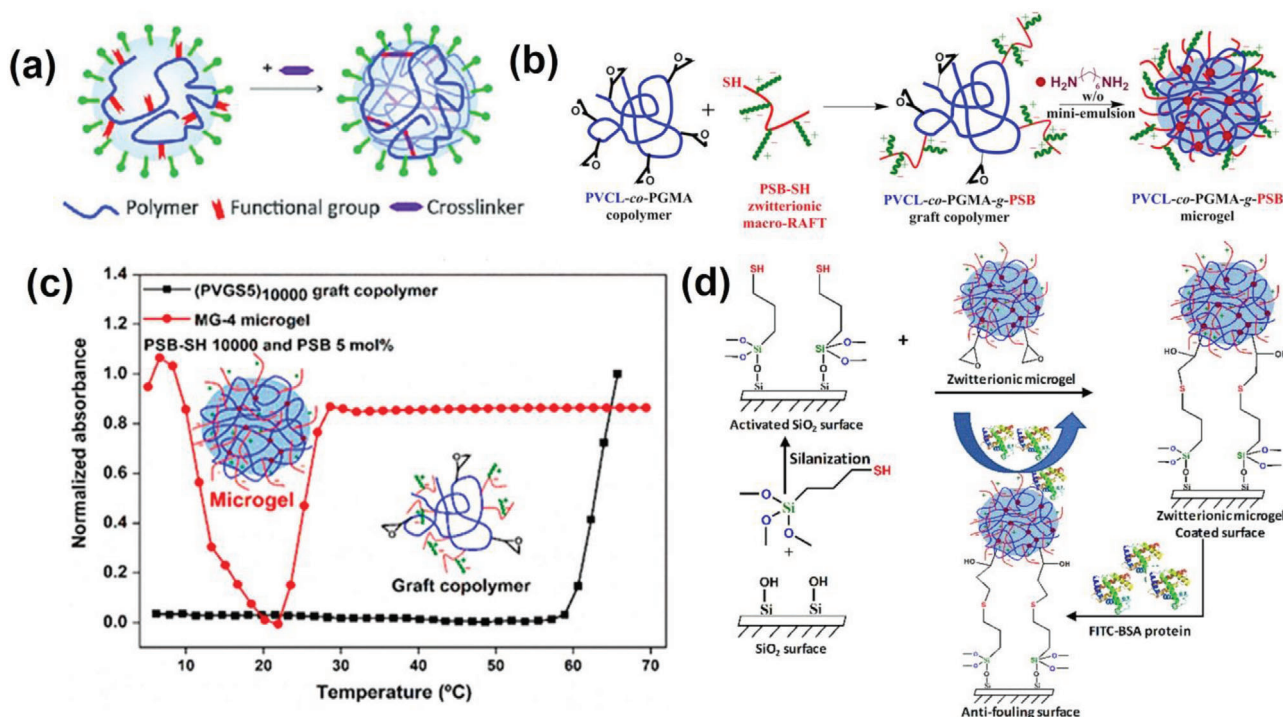


Figure 8. a) Schematic presentation of chemical cross-linking in the emulsion. Reproduced with permission.^[126] Copyright 2016, Royal Society of Chemistry. b) An example of zwitterionic microgel synthesis from a functional zwitterionic graft copolymer by the amine–epoxy crosslinking reaction in water droplets. c) Thermo-responsive behavior of the zwitterionic graft copolymer and microgel prepared with 5 mol% of PSB 10 000 g mol⁻¹ molecular weight thiol-functionalized polymer. d) Strategy to prepare the silica surface for antifouling performance with the microgels. Reproduced with permission.^[138] Copyright 2020, American Chemical Society.

utilized those nanogels for controlled release and real-time tracking of labeled dextran model drug.^[137]

2.5. Cross-Linking of Pre-Polymers in Emulsion Droplets

Other than the radical polymerization of mini-emulsified water droplets (containing monomer(s)), inverse mini-emulsion is also an ideal technique to produce microgels by cross-linking the functional groups present in the so-called nanoreactor water droplets (containing polymer(s)) with the help of a variety of functional cross-linkers (see **Figure 8a**).^[126] In this context, in our group, we have recently reported a dual-temperature sensitive zwitterionic microgel system with excellent antifouling activity. A poly(*N*-vinyl caprolactam-co-glycidyl methacrylate) (PVCL-co-PGMA) random copolymer was synthesized, followed by a partial molar consumption of the GMA groups (grafting to approach) with thiol-functionalized PSB zwitterionic pre-polymer, resulting in a hydrophilic graft copolymer. Finally, the cross-linking reaction (amine-epoxy) between zwitterionic PVCL-co-PGMA-g-PSB graft copolymer and 1,6-hexamethylene diamine cross-linker was carried out in water droplets of w/o mini-emulsion (see **Figure 8b**). The incorporation of such hydrophilic PSB zwitterionic chains increased the LCST of the graft copolymer drastically due to the formation of a stronger hydration layer around them (see **Figure 8c**). Interestingly, upon the conversion of the pre-polymer to the corresponding microgel, a UCST was observed along with an LCST in the single prototype (see **Figure 8c**). Also, the trace

amount of the GMA group serves the covalent attachment of the microgels on activated silica surface to perform the antifouling experiment with bovine serum albumin (BSA) model protein (see **Figure 8d**).^[138] In a similar approach, we also synthesized zwitterionic phosphobetaine (PMPC) microgels and showed for the first time their UCST behavior with varying PMPC chain length and semi-quantitatively measured their protein repellent behavior by X-ray photoelectron (XPS) studies.^[139]

3. Applications of Zwitterionic Nanogels and Microgels

Zwitterionic micro-and/or nanogels have found widespread applications in different fields due to their unique characteristics, such as high hydrophilicity, good biocompatibility, great tolerance to high saline, and thermo-responsiveness.^[140] Utilizing these unique features, the zwitterionic microgels can be used in the bio-medical field for controlled drug delivery in diabetes, cancer and tumor therapies, and bio-imaging of cancer cells.^[141–143] Also, they can be used as excellent coating materials to apply on several substrates to repel out different types of proteins and bacteria under harsh chemical and physical conditions. Moreover, the presence of oppositely charged groups inside the zwitterionic microgels makes them suitable to act as a nano-reactor to synthesize various metal nanoparticles as well.^[144]



3.1. Controlled Drug Delivery Systems for Tumor Therapy

In recent years, a variety of drug delivery systems have been developed to treat different diseases such as cancer and diabetes. For example, core-shell microgel, having a hydrophilic shell attached to the biological part and a hydrophobic core acting as a drug reservoir, is one of the efficient vectors for drug delivery, due to their high affinity to hydrophobic drugs like paclitaxel (PTX), and doxorubicin (DOX).^[145–147] The current stimuli-responsive micro-and/or nanogel systems based on amphiphilic (like PNIPAM, PVCL) polymers have been proved to be challenging in the drug delivery field due to their limited blood circulation time after systematic intravenous administration into the body because of nonspecific protein adsorption on the microgel particles from the blood. Protein aggregation and its denaturation on biological implants is a serious issue in the field of drug therapeutics.^[148] Protein adsorption generally leads to the formation of amyloid-like fibrils, which cause a wide range of diseases like Alzheimer's disease and Parkinson's disease.^[149,150] Therefore, the drug carrier (micro-and/or nanogel) must remain colloidally stable in blood for the successful and precise drug delivery to the targeted region and also, to achieve prolonged circulation in the blood, the microgels need to be modified with electrically neutral and highly hydrophilic materials. In this regard, zwitterionic micro-and/or nano gels, having very low immunogenicity and long life can reduce the foreign body reaction (FBR), also termed as the inflammatory reaction in vivo without being recognized by the macrophages due to their superior antifouling effect to resist nonspecific protein adsorption on their surfaces. Also, the zwitterionic materials used for the development of the nanogels are desirable to be quickly and completely degraded after the nanogels have achieved the targeted drug release, which diminishes the danger of unfavorable impacts brought by the non-degradable segments.^[151]

Because of the non-systemic bio-distribution and high cytotoxicity against normal cells, the administration of free anti-cancer drugs shows significant side effects. Now, targeting the specific cancer cells, stealth characteristics with enhanced blood circulation time, and controlled intracellular drug release at particular sites are the major requirements of an ideal anti-cancer drug delivery vector, which can improve the drug therapeutic efficacy and can also reduce the side effects. Nowadays, favorably biocompatible and ultra-low protein fouling zwitterionic nanogels are being accepted by researchers as novel anti-cancer drug carriers in clinical applications. The high cell viability (low cytotoxicity) of zwitterionic nanogels was first reported by Cheng and co-workers. They produced poly(carboxybetaine) (PCB) nanogels and utilized the abundance of the carboxylic groups to conjugate the ligand, cyclo[Arg-Gly-Asp-D-Tyr-Lys] (cRGD) to the PCB nanogels for targeted drug delivery.^[131] The cell viability assay was carried out seeding the Human umbilical cord vascular endothelial cells (HUVEC) in the presence of 3-(4,5-dimethylthiazol-2-yl)-2,5-diphenyltetrazolium bromide (MTT). The study shows (see Figure 9a) that the zwitterionic PCB nanogel synthesized by 3 mol% BIS cross-linker has high cell viability irrespective of the PCB nanogel concentrations and thereby proving themselves an excellent cellular uptake 3D polymer matrix. The intrinsic capacity toward the drug delivery of the PCB nanogels was also investigated, encapsulating FITC-labeled dextran drug by simple diffusion

without using any external stimuli such as temperature and pH. Almost 25% of the encapsulated FITC-dextran drug was released after 18 days because of the increase in their pore size due to the high hydrophilicity of the PCB nanogels. Also, flow cytometric study with HUVECs (at 37 °C) shows that the cRGD-conjugated nanogels loaded with FITC-dextran drug uptake higher HUVEC cell than the pure PCB nanogels without cRGD due to the capability of the cRGD ligand to bind a significant amount of HUVEC cells (see Figure 9b). Unlike the limitation of using conventional non-fouling functional groups (e.g., carboxylate-terminated poly(ethylene glycol) (PEG)) for the modification of the nanogel surfaces where the unreacted carboxylate groups could cause nonspecific protein adsorption,^[152] these ultrastable zwitterionic PCB nanogels serve as a multi-functional system to resist the nonspecific protein aggregation and also effectively uptake the cells for the targeted delivery of the drug-loaded. This kind of zwitterionic nanogel can be used as a potential platform for an anti-cancer drug delivery vector. Motivated by the findings of Cheng et al., Tian and co-workers fabricated a dual redox-responsive degradable zwitterionic nanogel system loaded with anti-cancer DOX drug for controlled release. The as-prepared nanogels were composed of poly(2-methacryloyloxyethyl phosphorylcholine) (PMPC) zwitterionic chains cross-linked with a novel diselenide (Se–Se) bond-containing *N,N'*-bis(acryloyl) selenocystamine (BMASC) cross-linker.^[125] In literature, a variety of diselenide bond-containing stimuli-triggered (such as oxidation, reduction, and γ -radiation) drug delivery systems have already been explored including micelles and metal–organic frameworks (MOFs) due to the lower bond energy of diselenide (Se–Se, 172 kJ mol⁻¹).^[153–155] The easily cleavable diselenide linkage makes the nanodrug carriers superior in redox-responsive degradation under mild chemical conditions. Owing to the unique dual redox-responsiveness (both oxidative and reductive), these types of diselenide-cross-linked nanogels particularly target the carcinogenic tumor cells where the reduced glutathione (GSH) concentration (≈ 10 mM) and level of H₂O₂ are much higher than the normal cells and the nanogels efficiently deliver the anti-cancer drug upon oxidative or reductive degradation. In the work of Tian et al., the use of zwitterionic PMPC chains in the nanogel strongly resists the nonspecific protein adsorption on the surface by virtue of its high antifouling characteristic. Hence, the nanogels exhibit a “stealth property” as well as circulate in the blood for a longer period without being rapidly cleared by the mononuclear phagocytosis system (MPS). The P(MPC–Se–Se–MPC) nanogels are capable of dual redox-responsive degradation in the presence of both GSH and H₂O₂ reductant and oxidant respectively. The disassembly of the nanogels is also H₂O₂ concentration-dependent because of the breaking of diselenide cross-linking sites in the nanogel, which could be seen by the step-like decrease in their turbidity measured by the DLS. Figure 9c shows that the higher the concentration of the H₂O₂, the faster is the rate of the nanogel degradation, for example, P(MPC–Se–Se–MPC)–25 (with 25 wt% of BMSAC diselenide cross-linker) nanogel shows a reduction in turbidity of 25.12% and 4.61% within 200 min at 0.01% and 0.1% H₂O₂, respectively.

Similarly, utilizing the low bond energy of disulfide (–S–S–), Men and co-workers also prepared reduction-responsive biodegradable poly(sulfobetaine methacrylate) (PSBMA) zwitterionic nanogels and used them as tumor-targeting delivery.

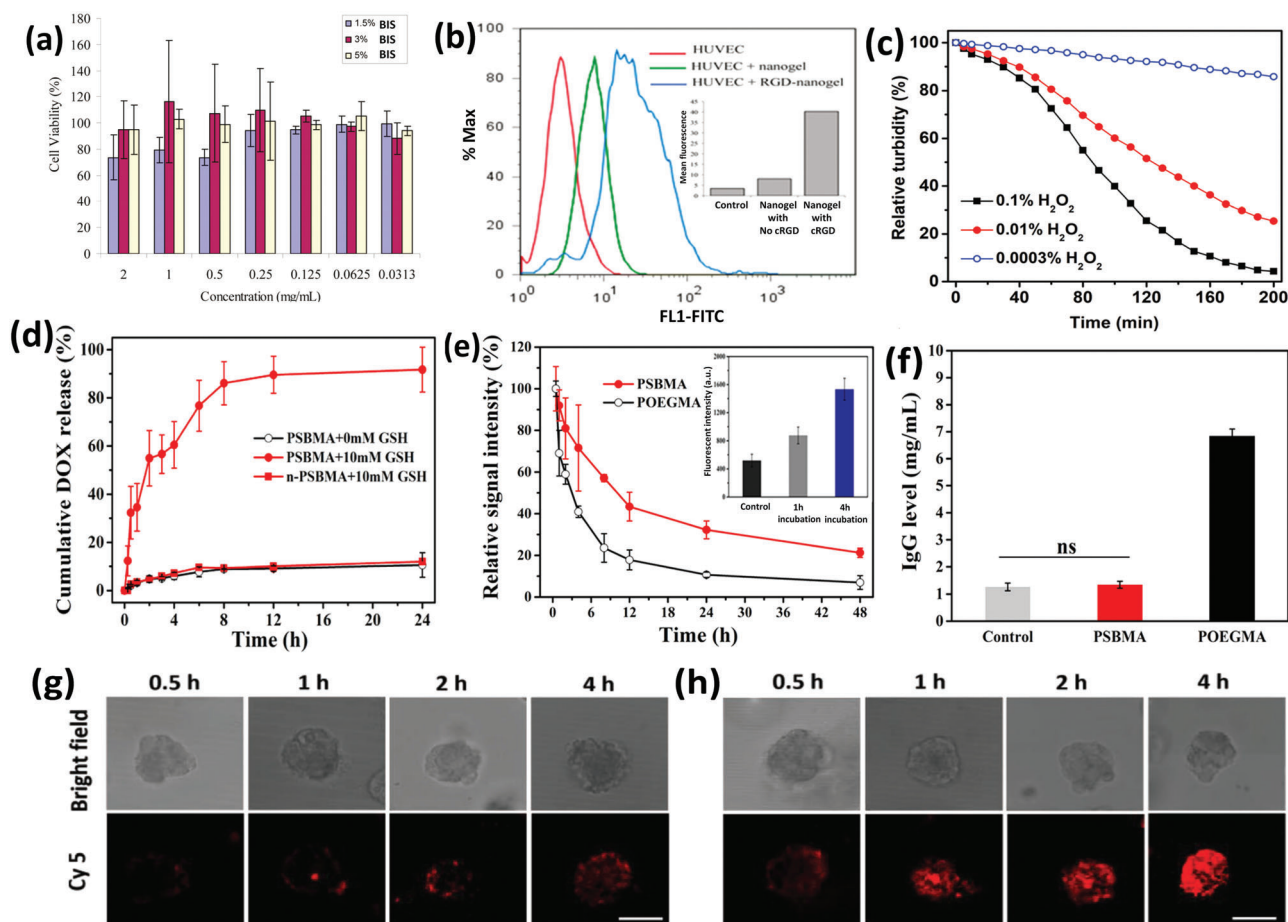


Figure 9. a) Cell viability of the PCB nanogels prepared at different BIS cross-linker concentration with human HUVEC cell. b) Flow cytometric analysis of the cellular uptake of PCB nanogels [5% BIS], red (no PCB nanogels); green (FITC-dextran loaded PCB nanogels); and blue (FITC-dextran loaded pCBMA nanogels conjugated with cRGD)]. Reproduced with permission.^[131] Copyright 2010, American Chemical Society. c) Oxidative degradation of P(MPC-Se-Se-MPC)-25 nanogel prepared with 25 wt% of BMSAC diselenide cross-linker in the presence of different H_2O_2 concentration. Reproduced with permission.^[125] Copyright 2020, Royal Society of Chemistry. d) DOX drug release from PSBA nanogel in the presence of different GSH concentrations under reductive degradation, where n-SBMA denotes nondegradable SBMA nanogels. e) In vivo blood retention profiles of POEGMA-Cy7.5 nanogels and PSBMA-Cy7.5 nanogels after the second injection in mice at a given dose of 1 mg mL^{-1} , f) IgG levels in the blood at the fifth day after the second injection of SBMA and POEGMA nanogels. Reproduced with permission.^[125] Copyright 2018, American Chemical Society. Penetration behaviors of transferrin (Tf)-modified PMEDAPA nanogels in HepG2 tumor spheroids at g) 37°C and h) 41°C . Scale bar 100 μm . Reproduced with permission.^[113] Copyright 2017, John Wiley & Sons.

Compared to the nondegradable PSBMA nanogels, these zwitterionic nanogels show a relatively faster release of DOX drug ($\approx 85\%$ in 12 h) under a reductive environment ($\approx 10 \text{ mM}$ GSH), suggesting that the drug release is highly accelerated by nanogel degradation (see Figure 9d). Moreover, the as-prepared PSBMA nanogels are highly noncytotoxic and uptake human hypopharyngeal carcinoma (FaDu) cells. Besides, the cellular uptake of drug-loaded PSBMA-DOX nanogels by FaDu cells was greatly increased with more incubation time due to the intracellular reduction condition (see inset of Figure 9e). It has been discussed earlier that, protein tends to bind to the surface of nanogels entering into the body called “protein corona,” which recognizes the nanogels as “foreign intruders” and eliminates them rapidly from the body. In this context, poly(oligo(ethylene glycol)methacrylate) (POEGMA) nanogels serve as a control platform for long blood circulation time due to the presence of poly(ethylene glycol) (PEG) units in POEGMA nanogels.^[156]

Nonetheless, Yang et al. observed that PEGylated gold nanoparticles (PEG-NPs) lost their long blood circulating capacity after repetitive injection into tumor-targeted cells in the same animal due to the production of immunoglobulin-G (IgG) antibodies to anti-PEG.^[157] Interestingly, the PSBMA nanogels labeled with Sulfo-Cyanine7.5 fluorophore (PSBMA-Cy7.5) exhibited a dramatically longer circulation time in blood than POEGMA-Cy7.5 even after injecting for the second time in the same mice blood system. Figure 9e shows that $\approx 21.3\%$ of PSBMA nanogels held into the blood, whereas only 6.7% of POEGMA nanogels were retained in the blood at 48 h even after the 7th day of the first injection, suggesting that PSBMA nanogels are much superior to PEGylated nanogel system. Besides, no significant increase in IgG antibody level in the mice treated on the 5th day of the second injection indicates the better stealth ability and the tumor accumulation of the PSBMA nanogels over POEGMA nanogels (see Figure 9f).

Without degrading the zwitterionic nanogels in a redox environment, they can also be used in tumor accumulation by simply augmenting the microwave. In this circumstance, Shen and co-workers were the first groups to develop cyto-compatible zwitterionic sulfamide-based PMEDAPA nanogels (see the chemical structure in Figure 2a) having UCST above the physiological temperature, where the zwitterionic nanogels responded to hyperthermia with the variation in cross-linker content (see Figure 2d,e).^[113] The PMEDAPA nanogels modified with transferrin (Tf) significantly penetrated HepG2 tumor spheroids manyfold stronger when incubated at 41 °C at 4 h than 37 °C. The PMEDAPA-Tf nanogels labeled with Cy-5 fluorophore at 41 °C are in fully swollen state and therefore, the Tf groups are mostly stretched outwards and interact with the Tf-receptors on the HepG2 tumor cell membranes, resulting in a stronger penetration ability and enhanced tumor cell uptake (see Figure 9g,h).

Despite the establishment of the cleavable cross-linkers in the fabrication of degradable nanogels under acidic, redox conditions with the controlled drug delivery in tumor treatment, another type of hypoxia-degradable nanogels has garnered much recognition from researchers in this field. Hypoxia with a reduced concentration of oxygen is a sign of almost all solid tumors, which results in an imbalance of redox state in the tumor, thereby enhancing the reductive stress. Various cleavable azobenzene derivatives have been developed to construct hypoxia-responsive drug nano-carriers. However, the hypoxia-responsive poly(phosphobetaine)-based degradable zwitterionic nanogel was first studied by Peng and co-workers. The synthesized nanogel exhibited negligible accelerated blood clearance (ABC) phenomenon along with the controlled release of DOX drug, resulting in a reduction of tumor weight in mice samples.^[158]

On the other hand, different types of amino acid-derived zwitterionic polymers (PAAZs) have been developed for drug-releasing, cancer diagnostic, and prolonged in vivo blood circulation by using their ultra-low fouling and functionalizing capabilities.^[159,160] In this context, Liu and co-workers reported the synthesis of poly(ornithine methacrylamide) (POrnAA) zwitterionic carboxybetaine-type nanogel with the help of a cross-linkable carbon dot (CCD) having exceptional photostability. While POrnAA served as a nonfouling drug-releasing vector, CCD functioned as both cross-linker and bio-imaging agent. Ultimately, they integrated this fluorescence active zwitterionic nanogel system toward the conjugation with folic acid (FA) as targeting ligand on their surfaces and those highly biocompatible FA-conjugated nanogels were internalized specifically by the cancer cells. Moreover, the FITC-labeled Dextran drug was released in the particular cancer cells and the activity of the nanogel during the controlled drug delivery was also monitored simultaneously by imaging.^[137]

3.2. Application as Colloidal Scaffolds or Templates for In Situ Metal Nanoparticle (MNP) Synthesis

Templates or scaffolds deriving out of several polymer matrices serve as a platform in the development of in vitro tissue models and in vivo regenerative medicinal treatments.^[161,162] Recently, microgels have been proved to be one of the promising matrices for cell migration, transportation of nutrients, and growth of

metal nanoparticles (MNPs) due to the presence of interstitial void spaces between the cross-linked building blocks with high porosity.^[27,163] In particular, microgels are better scaffolds over polymer microbeads in terms of achieving a higher number of nanoparticles (NPs) in their interior and also for more homogeneous distribution of the so-formed NPs in the microgel matrix.

Zwitterionic microgels are superhydrophilic due to the presence of both positive and negative charges within the same monomer repeating units that introduce a strong hydration layer at the microgel surface by electrostatic interaction with water and repel bacteria and protein adhesion strongly. Although the low-biofouling property of zwitterionic microgels resists the colonization of different micro-organisms on their surfaces, they cannot destroy the bacteria transmitted from the patients or the environment surrounding them.^[164] Therefore, incorporation of antibacterial agents, such as metal nanoparticles (MNPs) is highly desired into the zwitterionic microgel scaffold to completely prohibit the growth of bacteria colony, thereby combating wound inflammation.^[82] Generally, MNPs penetrate and disrupt the bacterial cell membrane by generating oxidative mechanical force, thus ultimately resulting in bacterial death.^[165] Besides offering a larger surface area, zwitterionic microgels not only favor a high concentration of metal ion-trapping but also can act as a microreactor for in situ synthesis of different MNPs due to their high structural stability by absorbing a large amount of water. Importantly, the control over the composition of the microgel network directly affects the size and shape of the MNPs. The aforementioned properties of polyzwitterions were first utilized by Das and co-workers for the microgel template-based synthesis of silver (Ag), gold (Au), and silver-gold (Ag–Au) bimetallic NPs.^[102] First, the synthesis of silver and gold NPs was carried out by sequestration of particular metal ions, that is, Ag^+ or AuCl_4^- ions in the interior of P(NIPAM-SB) zwitterionic microgel, followed by the reduction with sodium borohydride (NaBH_4). The presence of Ag and Au NPs before and after the synthesis of the inorganic hybrid microgel was detected by the UV–vis absorption spectra at 410 and 530 nm absorption peaks, respectively (see Figure 10a,b). Also, the Ag and Au NPs with 8–10 nm dimensional size was spotted in the microgel interior as shown by the respective transmission electron microscopic (TEM) images (see inset of Figure 10a,b). Additionally, the sequential addition of AuCl_4^- ions in the Ag nanoparticle-based hybrid microgel template led to the formation of Ag–Au bimetallic core-shell NPs. The trapping of AuCl_4^- ions both at the surface of Ag NPs and in the zwitterionic microgel interior (by NMe_3^+ ammonium ions) was well-characterized by the disappearance of the absorption peak of Ag NPs at 410 nm and a slight blue-shifting of Au NPs to 521 nm (see Figure 10c) even in the absence of NaBH_4 reducing agent. The strong oxidizing property of AuCl_4^- ions favors indeed the formation of elemental Au at the surface of Ag NPs by the redox reaction $3\text{Ag}(s) + \text{AuCl}_4^-(aq) \rightarrow \text{Au}(s) + 3\text{Ag}^+(aq) + 4\text{Cl}^-(aq)$. However, simultaneous addition of both AuCl_4^- and Ag^+ ions in the zwitterionic microgel template resulted in a gradual red-shifting of the single plasmonic band of Au NPs with an increasing molar ratio of AuCl_4^- , suggesting also the existence of alloy nature of the bimetallic silver–gold (Ag–Au) NPs. Another potential application of metal nanoparticles is heterogeneous catalysis. Without the use of appropriate catalysts, it is very difficult to carry out the reduction of various

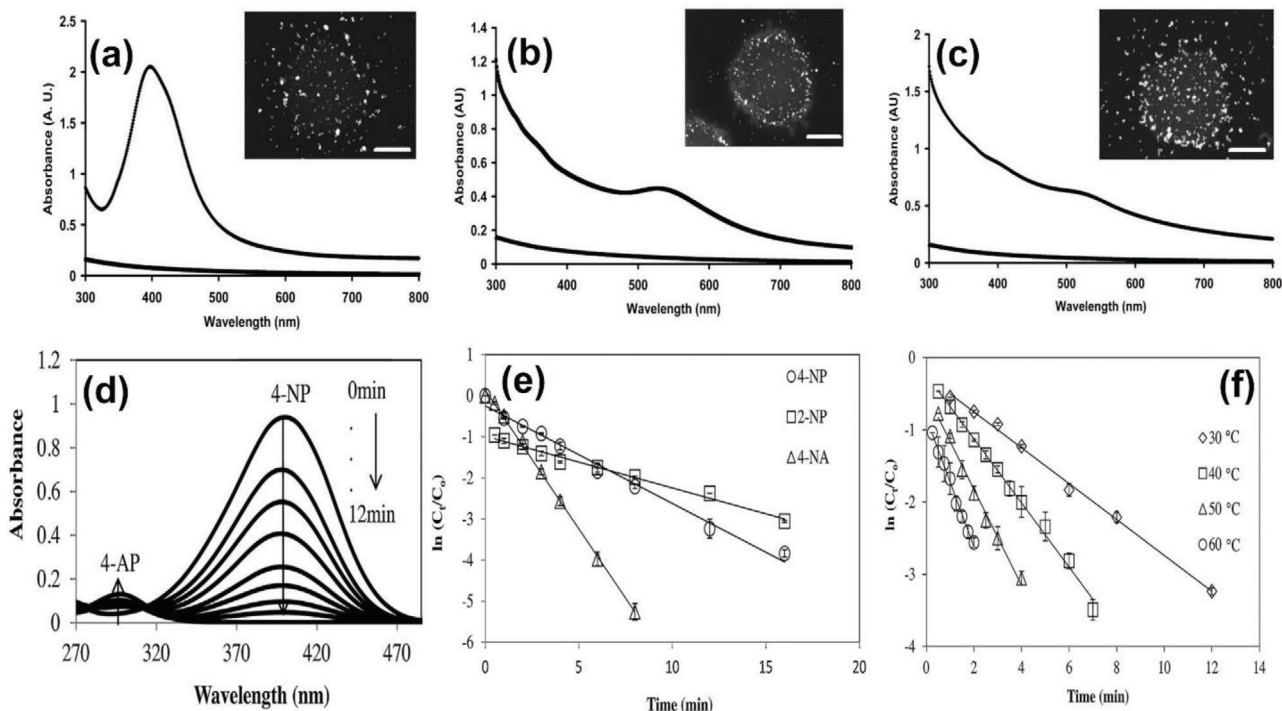


Figure 10. UV-vis absorbance spectra of the P(NIPAM-SB) zwitterionic microgels before (bottom spectra) and after template-based metal NP synthesis (top spectra): a) monometallic Ag NPs; b) monometallic Au NPs, c) bimetallic Au-Ag NP synthesis based on Ag NP incorporated P(NIPAM-SB) zwitterionic microgel template; the insets of the figures show the respective TEM images (scale bar 200 nm). Reproduced with permission.^[102] Copyright 2008, American Chemical Society. d) UV-vis absorbance spectra for the reduction of 4-nitrophenol (4-NP) over a time catalyzed by Ni NP loaded PSB zwitterionic microgel, e) kinetic plot of the reduction of 4-NP, 2-NP, and 4-NA catalyzed by PSB-Ni microgel composites against time at 30 °C, and f) kinetic plot of the reduction of 4-NP catalyzed by PSB-Ni microgel composites against time at different temperatures (30, 40, 50, and 60 °C). Reproduced with permission.^[132] Copyright 2015, Elsevier.

nitro-compounds into amines in a controlled manner, which is considered a very major organic reaction in the pharmaceutical industries.^[166] Recently, Ajmal and co-workers reported the synthesis of nickel (Ni) NPs in poly(sulfobetaine) (PSB) zwitterionic microgel template, where they exploited the catalytic activity of Ni NPs in the reduction of 4-nitrophenol (4-NP), 2-nitrophenol (2-NP), and 4-nitroaniline (4-NA) at different temperatures in the presence of NaBH_4 reducing agent.^[132] The steady decrease in the characteristic UV-vis absorption peak at 400 nm with time indicates that the 4-NP compound was reduced to the corresponding 4-amino phenol (4-AP) compound in the presence of Ni NP catalyst (see Figure 10d). They were also able to reuse the catalyst, Ni NP-loaded zwitterionic microgels after the reduction process, just by separating them from the reaction mixture and cleaning with deionized water. The molar excess (40-fold) use of NaBH_4 compared to the abovementioned nitro compounds does not have any significant effect on their reduction rate constant. Therefore, the catalytic efficacy of the Ni NP-loaded microgels was evaluated by a pseudo-first-order kinetic plot. Figure 10e shows the plot of $\ln(C_t/C_0)$ versus time, where C_0 is the initial concentration of the different nitro-compounds and C_t is the concentration of those nitro-compounds at a particular interval of times during the reduction process. Interestingly, the Ni NP microgel composite was found to be most effective in the reduction of 4-NA compound over the 4-NP and 2-NP nitro-compounds as the slope is much steeper in the case of the former than the latter ones.

Moreover, increasing the temperature also increased the rate of the reduction of the 4-NP compound linearly keeping the catalytic composition and other experimental conditions the same (see Figure 10f). An increase in the thermal energy results in the increased thermal motion of the polymer chains and due to that, the intra- and inter-polymer chain interaction between the opposite charges on the zwitterionic backbone becomes weaker. As a result, the zwitterionic polymer chains in the microgel network expand and the reactive species easily diffuse in the microgel interior to access the Ni NP catalysts. Furthermore, the anti-polyelectrolyte effect (i.e., swelling of polymer chains in salt solution by charge screening) of the so-prepared Ni NP microgel composites was also employed to determine their catalytic efficiency toward the reduction of the nitro-compounds.

3.3. Application as Coating and Membrane Materials

Over the years, zwitterionic polymers have mostly been used as coating materials, especially for biomedical applications. By virtue of their unique chemical nature, zwitterionic polymers are known to inhibit nonspecific protein adsorption. The presence of charges on the polymer backbone attracts the surrounding water molecules to form a strong hydration layer on the surface. This hydration layer, in turn, is responsible for keeping any biomolecules from getting adsorbed on the surface.

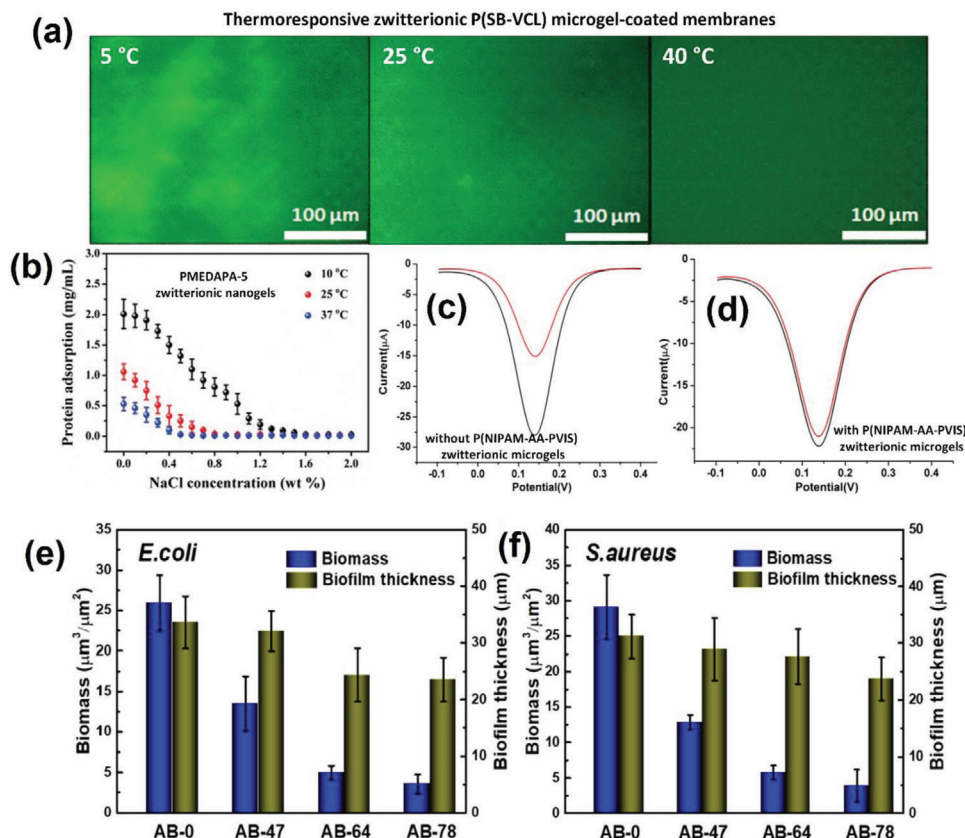


Figure 11. a) Fluorescence microscopic images of thermoresponsive P(SB-VCL) zwitterionic microgel-coated membranes at different temperatures, showing antifouling effect after the treatment with FITC-BSA (50 mg L^{-1}) solution (scale bar $100 \mu\text{m}$). Reproduced with permission.^[168] Copyright 2020, American Chemical Society. b) Plot of protein adsorption on zwitterionic PMEDAPA nanogels in water at various NaCl salt concentrations and different temperatures. Reproduced with permission.^[168] Copyright 2019, Royal Society of Chemistry. Differential pulse voltammetry (DPV) responses of the c) anti-STR/P(NIPAm-MPTC-GMA) microgels without zwitterionic content and d) the anti-STR/P(NIPAm-MPTC-GMA) microgels with P(NIPAM-AA-PVIS) zwitterionic microgels: before (red line) and after (black line); incubation in BSA protein solution (1 mg mL^{-1}). Reproduced with permission.^[114] Copyright 2019, American Chemical Society. Quantification of the biomass and thickness of the biofilms for AB-0, AB-47, AB-64, and AB-78 surfaces, respectively underflow condition e) *E. coli* bacteria and f) *S. aureus* bacteria, where AB-0, AB-47, AB-64, and AB-78 denote the weight ratio (in %) of the zwitterionic PSB/PES microgel in the surface. Reproduced with permission.^[120] Copyright 2020, American Chemical Society.

3.3.1. Anti-Fouling Coatings

Though zwitterionic polymers are known to provide nonspecific protein adsorption, quite interestingly zwitterionic microgels have been relatively less explored in this regard compared to other architectures such as linear chains, polymer brushes, and more. In a recent study in our group, we synthesized poly(*N*-vinylcaprolactam-co-sulfobetaine) (PSB-PVCL)-based core-shell microgels and they have shown that the presence of poly(sulfobetaine) (PSB) shell inhibits protein adsorption on the microgel surfaces in an efficient manner compared to pure Poly(*N*-vinylcaprolactam) microgels when coated on commercially available poly(ether sulfone) (PES) membranes.^[167] Interestingly, it was observed that at temperatures below the phase transition range of the PSB block, anti-fouling was relatively poorer, owing to the inability of the PSB chains to form a hydration layer due to their dipole-dipole induced collapsed conformation. This anti-fouling property was improved with increasing temperature as the PSB chains stretch out and can form hydrogen bonding with water, evident by the lack of fluores-

cence intensity from the FITC-BSA proteins (Figure 11a). The presence of NaCl salt also improved the anti-fouling property due to the anti-polyelectrolyte effect of the PSB block. In another interesting work, we synthesized PSB-functionalized microgels containing clickable poly(glycidyl methacrylate) (PGMA) repeat units, which enabled the resultant zwitterionic microgels to be covalently attached to activated surfaces like silica. The anti-fouling characteristics of these microgel-based coatings, in which the zwitterionic PSB repeat units were distributed uniformly across the microgel instead of just being at the shell, were shown to be highly efficient. Moreover, the attachment of BSA protein on the microgel coating was also quantified using a unique Quartz Crystal Microbalance-Dissipation (QCM-D) characterization technique.^[138] The dependence of the anti-fouling behavior of zwitterionic microgels on salt concentration was further corroborated by the findings of Peng and co-workers when the protein-repelling of PMEDAPA nanogels was observed to improve with a steady increase of NaCl salt concentration (Figure 11b). The said systems not only showed excellent protein-repelling under physiological conditions, but their anti-fouling

properties were also virtually unchanged even after multiple cycles of exposure to protein solutions.^[168] On the other hand, a very recent study by Banerjee and co-workers has shown that even when a zwitterionic component like poly(carboxybetaine) is present inside a cross-linked matrix of a microgel, the anti-fouling properties of the microgels are retained. Along with that, the presence of Rhodamine B-type fluorescence dye inside the microgel makes the system also equally important to trace the cancer cells for targeted drug delivery under an acidic environment.^[169]

The anti-fouling behavior of zwitterionic microgels has proved to be useful to enhance the sensitivity and detection limits of different antibiotics as well such as streptomycin (STR). He and co-workers synthesized microgels involving the zwitterionic component of Poly(1-propyl-3-vinylimidazole sulfonate) (PVIS) which in conjunction with comonomers like *N*-isopropylacrylamide (NIPAM) and acrylic acid (AA) show excellent protein-repellent behavior in complex media like uncured milk, thereby improving the sensitivity and detection limit of the particular antibiotic.^[114] In Figure 11c, it has been shown that electrodes coated with control samples (without zwitterionic functionalities), display a stark change in differential pulse voltammetry (DPV) current before and after incubation with BSA protein, compared to the electrodes coated with the zwitterionic microgels where the change in current is negligible. This is attributed to the fact that the absence of zwitterionic functionalities on the control electrodes leads to higher degrees of protein adsorption and that in return leads to significant changes in DPV signals. Rajan and co-workers have shown that this nonspecific protein repellent behavior also prevents thermal aggregation of proteins such as lysozyme and helps maintain their higher-order structure, which prevents neurodegenerative diseases in return.^[150]

3.3.2. Anti-Bacterial Applications

Bacterial adhesion and biofilm formation have traditionally been some of the most notorious issues that have plagued the biomedical industry such as surgical equipment, implants, and more. Besides proteins, the superhydrophilic nature of polyzwitterions has been useful to prevent bacterial adhesion on surfaces as well. According to a study by Huang and co-workers, it was observed that microgel films based on semi-interpenetrating networks (SIPN) between poly(ethersulfone) (PES) matrix and poly(sulfobetaine) (PSB) showed extremely low degrees of bacterial adhesion whereas pristine PES surfaces showed significant fouling owing to its relatively less hydrophilicity. It was observed that irrespective of whether the bacteria are gram-negative (*E.coli*) or gram-positive (*S.aureus*), with an increase in the amount of zwitterionic microgel on the casted surface, both the biomass and biofilm thickness decreased in a monotonic manner (Figure 11e,f).^[120] However, Sahiner and co-workers made an interesting and counter-intuitive observation while working with poly(ethylene imine) (PEI)-based microgels. When the PEI microgels were betainized (i.e., converted into a zwitterionic functionality) by the ring-opening with 1,3-propane sultone, the anti-bacterial efficiency diminished due to the conversion of the free amine groups to a positively charged ammonium species. Nonetheless, the biocompatibility was also increased following

this betainization which was confirmed by cytotoxicity assay studies.^[132]

3.3.3. Antifreezing and Antifogging Coatings

The formation of ice through frost or snow leads to extreme challenges for the durability of the infrastructures in daily life. Moreover, the accretion of ice causes, for example, the failure of transportation grids, the collapse of turbine blades by the natural gravity of ice.^[170] On the other hand, the uneven condensation of water droplets on a transparent surface results in the formation of fog that effectively diminishes the transparency of the surface. The main strategy to mitigate these freezing and fogging problems is to tune the wettability of the transparent surface either chemically (deposition of different materials via coating) or physically (modifying the surface roughness). According to the antifreezing and antifogging mechanism, the hydrophilic type coating materials have widely been researched in recent years.^[171] In principle, due to the low contact angle between the water droplet and hydrophilic substrate, the surface hydration layer resists further water condensation or fog formation. In this sense, zwitterionic polymers have been reported in literature, owing to their superhydrophilicity because of the presence of both cation and anion on their backbone. The coating of such hydrophilic material by grafting on the activated glass surface resulted in excellent antifogging and antifreezing performances. However, the utilization of such hydrophilic materials in the form of microgel is much more advantageous over these 'grafting to' or 'grafting from' methods because of their relatively easy and fast deposition to obtain highly dense coating, control over layer thickness by tuning the microgel size, and also by incorporating various comonomers of different functionalities. Such kind of antifreezing and antifogging applications are rarely exercised in literature and taking that into consideration, Varnoozfaderani and co-workers are the first group to prepare a durable microgel-based antifreezing coating of poly(sulfobetaine-co-dopamine methacrylamide), P(SB-DOPA)).^[172] Here, the presence of dopamine moiety, having excellent adhesive property helped them to achieve a universal coating with a wide range of substrates. In their study, the authors have suggested that being polyzwitterions in the microgel matrix enabled film formations, which were resistant to freezing and fogging. The superhydrophilic nature of the polyzwitterion reduces the water contact angle to such an extent, that condensation of vapor is prevented. Also, the formation of frost was largely prohibited by the thick hydration layer of zwitterionic microgels. It was shown that microgels with lower cross-link density were softer and could cover the surface more efficiently by spreading out, leading to better results concerning antifreezing and antifogging performance (Figure 12a,b).

3.3.4. Removal of Pollutants from Water

At the offshore platform, accidental leakage of oil frequently occurs during crude oil transportation, which allows a significant volume of oil to flood the oceans. Dispersed oil, free oil, and emulsified oil are mainly the three different types of oil in this regard. While it is possible to clean the free oil and dispersed

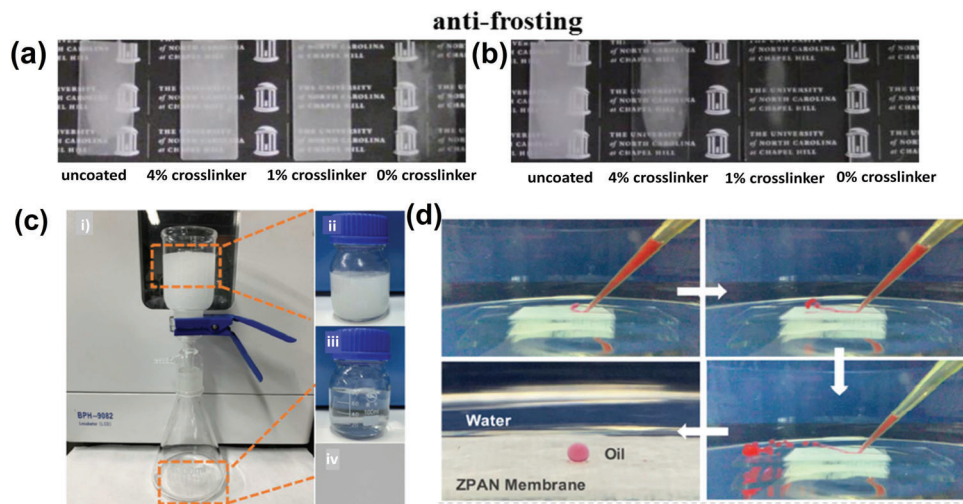


Figure 12. Antifrosting performance: a) the uncoated and coated glass slides with microgels containing 0, 1, and 4 mol% cross-linker were exposed to 85% relative humidity for 3 h followed by quick cooling to -20°C for 2 h to freeze the absorbed water on the slides and b) exposure to ambient condition for 1 min. Ice on the coated slides melted while the ice remained on the uncoated slide. Reproduced with permission.^[172] Copyright 2018, American Chemical Society. Water–oil separation performance: c) dynamic photographs of i) the filtration apparatus, ii) the oil-in-water emulsion, iii) the corresponding filtrate, and iv) optical microscopy image of the filtrate, and d) dynamic photographs of underwater anti-oil-adhesive performance of the zwitterionic nanogel-treated PAN (ZPAN) membrane. Reproduced with permission.^[177] Copyright 2020, Elsevier.

oil mechanically, emulsified oil with smaller droplets (size between 10 and 20 μm) is very challenging to eliminate by conventional water treatment procedures, for example, flocculation and chemical coagulation.^[173,174] However, researchers have been able to come up with a novel membrane-based separation technique together with nano- and/or ultra-filtration and due to its high separation efficiency, low risk of secondary pollution, and cost-effectiveness, it has attracted much attention in recent days. In particular, when the conventional “size-sieving” membranes are treated with surfactant-stabilized emulsions, the oil droplets get adsorbed on the membrane surface via electrostatic interaction and thereby reduce the workability of the membranes to separate water from oil-in-water (o/w) emulsion. Therefore, a variety of super-wetting materials has been proposed in literature to enhance the antifouling activity and separation efficiency of o/w emulsions. Generally, when the membrane surface is functionally modified by super hydrophilic groups, it can absorb a large number of water molecules and form a strong hydration layer that effectively prevents the oil droplets from getting wet on the membrane underwater. In this context, polyzwitterionic micro- and/or nanogels have also been considered as a superior material for water treatment from o/w emulsions.^[175,176] In a recent study, Zang and co-workers have shown that the superhydrophilic nature of polyzwitterions renders them to be superoleophobic especially in underwater conditions. Poly(sulfobetaine)-based microgels were prepared and grafted on poly(acrylonitrile) (PAN) membranes, which showed extremely low water contact angle and extremely high oil contact angles irrespective of the salt concentration and solution pH.^[177] It was observed that the superhydrophilicity provided free passage to the water molecules across the membrane, thereby leading to efficient oil–water separation from a stable emulsion (Figure 12c). On the other hand, when the zwitterionic microgel-grafted PAN (ZPAN) membranes were exposed to different oil–water emulsions, the superoleophobicity

of the membranes led the oil droplets to roll on the membrane’s surface and coalesce leading to demulsification (Figure 12d).

Organic dyes are the most detrimental contaminants found in industrial wastewater, and are a threat to human health and living organisms. Nowadays, adsorption is the most commonly employed and efficient technique to remove organic dyes from water. In the previously discussed work by Sahiner and co-workers, the authors have shown that besides improving the biocompatibility of poly(ethylene imine) (PEI) microgels, betainization (conversion to a zwitterionic derivative) enables the separation of differently charged organic dyes as well.^[98] It was observed that the presence of both positive and negative charges in the betainized version of the microgels renders them net positive at acidic pHs and net negative at alkaline pHs. This property was exploited to separate the methylene orange (negatively charged) and methylene blue (positively charged, see Figure 1b), respectively. Since the extent of negatively charged in the betainized version of the microgels was far greater than the nonbetainized PEI microgels, consequently the efficacy of separation of methylene blue was much better for the betainized versions at alkaline pH. The authors have proposed that these microgel prototypes might be useful for applications such as wastewater treatment.

4. Conclusion and Future Perspectives

Briefly, this minireview delineates the recent advances in the development of zwitterionic nanogels and microgels for different potential applications. We first summarized the several synthesis routes to fabricate the zwitterionic polybetaine nanogels and microgels (e.g., aqueous and nonaqueous precipitation polymerization, emulsion polymerization in water droplets, and post-modification of other functional nanogels) and then emphasized the various works done in this particular field, highlighting a few of our contributions as well. The easy and straightforward

synthesis techniques of these functional zwitterionic microgels broaden the range of variables for the tuning of their solution properties (e.g., thermo- and salt-responsiveness) and differentiate them distinctly from other polymeric architectures when used for similar applications. We discussed that the specific application of the microgels as advanced materials critically depends on the design of the type of the zwitterionic and other comonomeric units. Zwitterionic polymers are classified as fascinating materials owing to their high biodegradability and biocompatibility. In combination with these properties, the produced zwitterionic micro-and/or nanogels have found interesting applications in biomedical field, such as cancer and tumor therapy. In this regard, their excellent anti-bioadhesion property makes them highly nonimmunogenic and advantageous for timely drug discharge in targeted drug delivery system. On the other hand, their protein-repelling property due to the superhydrophilicity serves a platform to engineer different kinds of coatings,^[61] for example, antifouling, antibacterial, and antifrosting as well as designing smart membranes for wastewater treatment. The prevalence of both positive and negative charges in the zwitterionic microgel interior endorses them into emerging colloidal scaffolds for the synthesis of metal nanoparticles that help to formulate the antibacterial pharmaceuticals, also covered in this minireview.

Nonetheless, the synthesis of novel types of zwitterionic microgels from nonconventional zwitterionic betaine monomers still needs to be explored.^[77] The high incorporation of the zwitterionic units in the corresponding microgels having assymetrical morphology (e.g., Janus type) is still a challenging factor and can be improved by optimizing different synthesis approaches, such as via synthesizing zwitterionic macromonomers using different polymerization methods. This might help in lowering the protein adsorption and improve antifouling properties (restricted biofilm formation) largely, thereby increasing the longer blood circulation time of drug carriers and increasing the life-time of medical devices. Furthermore, various stimuli-responsive functionalities (e.g., glycopeptides) can be instituted judiciously into the zwitterionic nanogels to stimulate cells by chemical (e.g., pH) or physical (e.g., ultrasound and light) triggers that have not been extensively explored in the existing literature.^[178,179,180] To produce ultrastable antifouling membranes constituted of zwitterionic microgels operating in harsh physical or chemical conditions, such as high temperature and variable pH, and separating heavy metal ions from industrial wastewater, are the future challenges for membrane researchers and engineers. Zwitterionic microgels are very promising materials in terms of membrane application and they should be brought to large-scale uses soon. One aspect could be the casting of membrane sheets directly from the zwitterionic microgel solution at variable temperature and pH in a batch process. We envision that this focused minireview will be beneficial for a broad readership to understand the further improvement on the zwitterionic nanogels and microgels based on their state of the art.

Acknowledgements

The authors would like to acknowledge Deutsche Forschungsgemeinschaft, Germany (DFG) (grant no. PI 614/9-1) and Department of Science and Technology, India (DST) (grant no. INT/FRG/DFG/P-04/2017) for the funding of this project under the DFG-DST joint collaborative framework.

Open access funding enabled and organized by Projekt DEAL.

Conflict of Interest

The authors declare no conflict of interest.

Keywords

antifouling, colloidal stability, microgels, nanogels, stimuli-responsiveness, swelling, zwitterions

Received: February 22, 2021

Revised: April 24, 2021

Published online: May 22, 2021

- [1] D. Klinger, K. Landfester, *Polymer* **2012**, *53*, 5209.
- [2] J. K. Oh, R. Drumright, D. J. Siegwart, K. Matyjaszewski, *Prog. Polym. Sci.* **2008**, *33*, 448.
- [3] Y. Li, D. Maciel, J. Rodrigues, X. Shi, H. Tomás, *Chem. Rev.* **2015**, *115*, 8564.
- [4] R. L. Juliano, X. Ming, O. Nakagawa, *Bioconjugate Chem.* **2012**, *23*, 147.
- [5] G. Agrawal, R. Agrawal, A. Pich, *Part. Part. Syst. Charact.* **2017**, *34*, 1700132.
- [6] H. G. Schild, D. A. Tirrell, *J. Phys. Chem.* **1990**, *94*, 4352.
- [7] F. A. Plamper, W. Richtering, *Acc. Chem. Res.* **2017**, *50*, 131.
- [8] J. Ramos, A. Imaz, J. Forcada, *Polym. Chem.* **2012**, *3*, 852.
- [9] M.-N. Birkholz, G. Agrawal, C. Bergmann, R. Schröder, S. J. Lechner, A. Pich, H. Fischer, *Biomed. Eng.* **2016**, *61*, 267.
- [10] G. Agrawal, M. P. Schürings, P. Van Rijn, A. Pich, *J. Mater. Chem. A* **2013**, *1*, 13244.
- [11] S. Neyret, B. Vincent, *Polymer* **1997**, *38*, 6129.
- [12] T. Hoare, R. Pelton, *Macromolecules* **2004**, *37*, 2544.
- [13] A. Fernández-Nieves, A. Fernández-Barbero, F. J. D. e. L. Nieves, B. Vincent, *J. Phys.: Condens. Matter* **2000**, *12*, 3605.
- [14] S. Dai, P. Ravi, K. C. Tam, *Soft Matter* **2008**, *4*, 435.
- [15] M. Heskins, J. E. Guillet, *J. Macromol. Sci., Part A: Chem.* **1968**, *2*, 1441.
- [16] M. Irie, *Pure Appl. Chem.* **1990**, *62*, 1495.
- [17] T. Sawai, S. Yamazaki, Y. Ishigami, Y. Ikariyama, M. Aizawa, *J. Electroanal. Chem.* **1992**, *322*, 1.
- [18] A. Fernández-Nieves, M. Márquez, *J. Chem. Phys.* **2005**, *122*, 084702.
- [19] R. Schroeder, A. A. Rudov, L. A. Lyon, W. Richtering, A. Pich, I. I. Potemkin, *Macromolecules* **2015**, *48*, 5914.
- [20] M. Motornov, Y. Roiter, I. Tokarev, S. Minko, *Prog. Polym. Sci.* **2010**, *35*, 174.
- [21] I. Neamtu, A. G. Rusu, A. Diaconu, L. E. Nita, A. P. Chiriac, *Drug Delivery* **2017**, *24*, 539.
- [22] A. K. Bajpai, S. K. Shukla, S. Bhanu, S. Kankane, *Prog. Polym. Sci.* **2008**, *33*, 1088.
- [23] M. Karg, A. Pich, T. Hellweg, T. Hoare, L. A. Lyon, J. J. Crassous, D. Suzuki, R. A. Gumerov, S. Schneider, I. I. Potemkin, W. Richtering, *Langmuir* **2019**, *35*, 6231.
- [24] Y. L. Colson, M. W. Grinstaff, *Adv. Mater.* **2012**, *24*, 3878.
- [25] Y. Wang, Q. Luo, W. Zhu, X. Li, Z. Shen, *Polym. Chem.* **2016**, *7*, 2665.
- [26] L. Fass, *Mol. Oncol.* **2008**, *2*, 115.
- [27] J. Zhang, S. Xu, E. Kumacheva, *J. Am. Chem. Soc.* **2004**, *126*, 7908.
- [28] S. Maji, B. Cesur, Z. Zhang, B. G. De Geest, R. Hoogenboom, *Polym. Chem.* **2016**, *7*, 1705.
- [29] M. L. Zheludkevich, J. Tedim, M. G. S. Ferreira, *Electrochim. Acta* **2012**, *82*, 314.
- [30] T. Lohaus, P. De Wit, M. Kather, D. Menne, N. E. Benes, A. Pich, M. Wessling, *J. Membr. Sci.* **2017**, *539*, 451.

- [31] D. Menne, F. Pitsch, J. E. Wong, A. Pich, M. Wessling, *Angew. Chem., Int. Ed.* **2014**, *53*, 5706.
- [32] V. Vladimir, F. Winnik, *Nat. Mater.* **2010**, *9*, 101.
- [33] R. Keidel, A. Ghavami, D. M. Lugo, G. Lotze, O. Virtanen, P. Beumers, J. S. Pedersen, A. Bardow, R. G. Winkler, W. Richtering, *Sci. Adv.* **2018**, *4*, eaao7086.
- [34] A. K. Yetisen, H. Butt, L. R. Volpatti, I. Pavlichenko, M.ž Humar, S. J. J. Kwok, H. Koo, K. I. S. u Kim, I. Naydenova, A. Khademhosseini, S. K. Hahn, S. H. Yun, *Biotechnol. Adv.* **2016**, *34*, 250.
- [35] N. M. B. Smeets, T. Hoare, *J. Polym. Sci., Part A: Polym. Chem.* **2013**, *51*, 3027.
- [36] M. Das, H. Zhang, E. Kumacheva, *Annu. Rev. Mater. Res.* **2006**, *36*, 117.
- [37] A. V. Kabanov, S. V. Vinogradov, *Angew. Chem., Int. Ed.* **2009**, *48*, 5418.
- [38] Y. Okada, F. Tanaka, *Macromolecules* **2005**, *38*, 4465.
- [39] G. Charlet, G. Delmas, *Polymer* **1981**, *22*, 1181.
- [40] H. Feil, Y. H. Bae, J. Feijen, S. W. Kim, *Macromolecules* **1993**, *26*, 2496.
- [41] E. Mueller, R. J. Alsop, A. Scotti, M. Bleucl, M. C. Rheinstädter, W. Richtering, T. Hoare, *Langmuir* **2018**, *34*, 1601.
- [42] M. Brugnoni, A. Scotti, A. A. Rudov, A. P. H. Gelissen, T. Caumanns, A. Radulescu, T. Eckert, A. Pich, I. I. Potemkin, W. Richtering, *Macromolecules* **2018**, *51*, 2662.
- [43] A. J. Schmid, J. Dubbert, A. A. Rudov, J. S. Pedersen, P. Lindner, M. Karg, I. I. Potemkin, W. Richtering, *Sci. Rep.* **2016**, *6*, 22736.
- [44] M. Cors, O. Wrede, A.-C. Genix, D. Anselmetti, J. Oberdisse, T. Hellweg, *Langmuir* **2017**, *33*, 6804.
- [45] L. Etchenausia, E. Deniau, A. Brûlet, J. Forcada, M. Save, *Macromolecules* **2018**, *51*, 2551.
- [46] M. Kather, F. Ritter, A. Pich, *Chem. Eng. J.* **2018**, *344*, 375.
- [47] H. J. M. Wol, M. Kather, H. Breisig, W. Richtering, A. Pich, M. Wessling, *ACS Appl. Mater. Interfaces* **2018**, *10*, 24799.
- [48] S. Deshpande, S. Patil, N. Singh, *ACS Omega* **2018**, *3*, 8042.
- [49] Y. Matsuda, M. Kobayashi, M. Annaka, K. Ishihara, A. Takahara, *Langmuir* **2008**, *24*, 8772.
- [50] C. Hang, Y. Zou, Y. Zhong, Z. Zhong, F. Meng, *Colloids Surf., B* **2017**, *158*, 547.
- [51] G. Romeo, L. Imperiali, J.-W. Kim, A. Fernández-Nieves, D. A. Weitz, *J. Chem. Phys.* **2012**, *136*, 124905.
- [52] C. Pellet, M. Cloitre, *Soft Matter* **2016**, *12*, 3710.
- [53] E. Mihalko, K. e Huang, E. Sproul, K. e Cheng, A. C. Brown, *ACS Nano* **2018**, *12*, 7826.
- [54] A. R. Town, M. Giardiello, R. Gurjar, M. Siccardi, M. E. Briggs, R. Akhtar, T. O. Mcdonald, *Nanoscale* **2017**, *9*, 6302.
- [55] K. C. Clarke, S. N. Dunham, L. A. Lyon, *Chem. Mater.* **2015**, *27*, 1391.
- [56] C. S. Hayes, B. Bose, R. T. Sauer, *J. Biol. Chem.* **2002**, *277*, 33825.
- [57] L.-J. Wang, X.-D. Kong, H.-Y. Zhang, X.-P. Wang, J. Zhang, *Biochem. Biophys. Res. Commun.* **2000**, *276*, 346.
- [58] J. Menzie, H. Prentice, J.-Y. Wu, *Brain Sci.* **2013**, *3*, 877.
- [59] A. Acids, H. B. Vickery, C. L. A. Schmidt, *Chem. Rev.* **1931**, *9*, 169.
- [60] M. Ilčiková, J. Tkáč, P. Kasák, *Polymers* **2015**, *7*, 2344.
- [61] L. D. Blackman, P. A. Gunatillake, P. Cass, K. E. S. Locock, *Chem. Soc. Rev.* **2019**, *48*, 757.
- [62] M. Hess, R. G. Jones, J. Kahovec, T. Kitayama, P. Kratochvíl, P. Kubisa, W. Mormann, R. F. T. Stepto, D. Tabak, J. Vohlidal, E. S. Wilks, *Pure Appl. Chem.* **2006**, *78*, 2067.
- [63] E. Ruoslahti, M. D. Pierschbacher, *Cell* **1986**, *44*, 517.
- [64] N. Bonte, A. Laschewsky, *Polymer* **2019**, *37*, 2011.
- [65] C. Alvarez-Lorenzo, H. Hiratani, K. Tanaka, K. Stancil, A. Y. u. Grosberg, T. Tanaka, *Langmuir* **2001**, *17*, 3616.
- [66] Y. M. Mohan, K. E. Geckeler, *React. Funct. Polym.* **2007**, *67*, 144.
- [67] H. Yu, D. W. Grainger, *J. Appl. Polym. Sci.* **1993**, *49*, 1553.
- [68] W. Xu, A. Rudov, A. Oppermann, S. Wypysek, M. Kather, R. Schroeder, W. Richtering, I. I. Potemkin, D. Wöll, A. Pich, *Angew. Chem., Int. Ed.* **2020**, *59*, 1248.
- [69] W. Xu, A. Rudov, R. Schroeder, I. V. Portnov, W. Richtering, I. I. Potemkin, A. Pich, *Biomacromolecules* **2019**, *20*, 1578.
- [70] K. Ogawa, A. Nakayama, E. Kokufuta, *Langmuir* **2003**, *19*, 3178.
- [71] W. Cai, R. B. Gupta, *J. Appl. Polym. Sci.* **2003**, *88*, 2032.
- [72] S. Kudaibergenov, W. Jaeger, A. Laschewsky, *Adv. Polym. Sci.* **2006**, *201*, 157.
- [73] J. M. Knipe, F. Chen, N. A. Peppas, *J. Appl. Polym. Sci.* **2014**, *131*, 1.
- [74] J. Kötz, B. Paulke, B. Philipp, P. Denkinger, W. Burchard, *Acta Polym.* **1992**, *43*, 193.
- [75] J. E. Wong, A. M. Díez-Pascual, W. Richtering, *Macromolecules* **2009**, *42*, 1229.
- [76] X. Hu, Z. Tong, L. A. Lyon, *Colloid Polym. Sci.* **2011**, *289*, 333.
- [77] A. Laschewsky, *Polymers* **2014**, *6*, 1544.
- [78] Z. Xiong, Y. Wang, J. Zhu, X. Li, Y. He, J. Qu, M. Shen, J. Xia, X. Shi, *Nanoscale* **2017**, *9*, 12295.
- [79] X. Li, S. Lu, Z. Xiong, Y. Hu, D. Ma, W. Lou, C. Peng, M. Shen, X. Shi, *Adv. Sci.* **2019**, *6*, 1901800.
- [80] S. Sugihara, K. Sugihara (Nee Nishikawa), S. P. Armes, H. Ahmad, A. L. Lewis, *Macromolecules* **2010**, *43*, 6321.
- [81] E. S. Jeong, H. A. Son, M. K. Kim, K.-H. Park, S. Kay, P. S. Chae, J. W. Kim, *Colloids Surf., B* **2014**, *123*, 339.
- [82] P. Wang, J. Yang, B. Zhou, Y. Hu, L. Xing, F. Xu, M. Shen, G. Zhang, X. Shi, *ACS Appl. Mater. Interfaces* **2017**, *9*, 47.
- [83] J. Liu, Z. Xiong, J. Zhang, C. Peng, B. Klajnert-Maculewicz, M. Shen, X. Shi, *ACS Appl. Mater. Interfaces* **2019**, *11*, 15212.
- [84] H. Ahmad, D. Dupin, S. P. Armes, A. L. Lewis, *Langmuir* **2009**, *25*, 11442.
- [85] Z. Li, H. Li, Z. Sun, B. Hao, T.-C. Lee, A. Feng, L. Zhang, S. H. Thang, *Polym. Chem.* **2020**, *11*, 3162.
- [86] O. Azzaroni, A. A. Brown, W. T. S. Huck, *Angew. Chem., Int. Ed.* **2006**, *118*, 1802.
- [87] N. Nizarod, D. Schanzenbach, E. Schönemann, A. Laschewsky, *Polymers* **2018**, *10*, 325.
- [88] Z. Li, B. Hao, Y. Tang, H. Li, T.-C. Lee, A. Feng, L. Zhang, S. H. Thang, *Eur. Polym. J.* **2020**, *132*, 109704.
- [89] J. Niskanen, H. Tenhu, *Polym. Chem.* **2017**, *8*, 220.
- [90] F. Xuan, J. Liu, *Polym. Int.* **2009**, *58*, 1350.
- [91] S. Jiang, Z. Cao, *Adv. Mater.* **2010**, *22*, 920.
- [92] M. Binazadeh, M. Kabiri, L. D. Unsworth in *Proteins at Interfaces III State of the Art* (Eds: T. Horbett, J. L. Brash, W. Norde), ACS Symposium Series, Vol. 1120, American Chemical Society, Washington, DC **2012**, Ch. 28.
- [93] L. R. Carr, Y. Zhou, J. E. Krause, H. Xue, S. Jiang, *Biomaterials* **2011**, *32*, 6893.
- [94] P. Zhang, F. Sun, C. Tsao, S. Liu, P. Jain, A. Sinclair, H.-C. Hung, T. Bai, K. Wu, S. Jiang, *Proc. Natl. Acad. Sci. USA* **2015**, *112*, 12046.
- [95] B. H. Tan, P. Ravi, K. C. Tam, *Macromol. Rapid Commun.* **2006**, *27*, 522.
- [96] K. A. Gunay, P. Theato, H. A. Klok, in *Functional Polymers by Post-Polymerization Modification* (Eds: Dr. P. Theato, Prof. H.-A. Klok), Wiley-VCH, Weinheim, Germany **2013**, Ch. 1.
- [97] M. A. Gauthier, M. I. Gibson, H.-A. Klok, *Angew. Chem., Int. Ed.* **2009**, *48*, 48.
- [98] N. Sahiner, S. Demirci, *Mater. Sci. Eng., C* **2017**, *77*, 642.
- [99] A. Sinclair, M. B. O'Kelly, T. Bai, H.-C. Hung, P. Jain, S. Jiang, *Adv. Mater.* **2018**, *30*, 1803087.
- [100] F. A. L. Janssen, M. Kather, L. C. Kröger, A. Mhamdi, K. Leonhard, A. Pich, A. Mitsos, *Ind. Eng. Chem. Res.* **2017**, *56*, 14545.
- [101] A. Melle, A. Balaceanu, M. Kather, Y. Wu, E. Gau, W. Sun, X. Huang, X. Shi, M. Karperien, A. Pich, *J. Mater. Chem. B* **2016**, *4*, 5127.
- [102] M. Das, N. Sanson, E. Kumacheva, *Chem. Mater.* **2008**, *20*, 7157.
- [103] W. Xue, S. Champ, M. B. Huglin, *Eur. Polym. J.* **2001**, *37*, 869.
- [104] R. B. Koizhaiganova, V. B. Sigitov, L. A. Bimendina, S. E. Kudaibergenov, *Polym. Bull.* **2005**, *53*, 161.

- [105] A. J. Schmid, R. Schroeder, T. Eckert, A. Radulescu, A. Pich, W. Richtering, *Colloid Polym. Sci.* **2015**, 293, 3305.
- [106] H. Yoshimitsu, E. Korchagina, A. Kanazawa, S. Kanaoka, F. M. Winnik, S. Aoshima, *Polym. Chem.* **2016**, 7, 2062.
- [107] S. Liu, S. P. Armes, *Angew. Chem., Int. Ed.* **2002**, 41, 1413.
- [108] M. Arotçaréna, B. Heise, S. Ishaya, A. Laschewsky, *J. Am. Chem. Soc.* **2002**, 124, 3787.
- [109] R. Rajan, K. Matsumura, *Macromol. Rapid Commun.* **2017**, 38, 1700478.
- [110] P. Saha, M. Kather, S. L. Banerjee, N. K. Singha, A. Pich, *Eur. Polym. J.* **2019**, 118, 195.
- [111] V. Hildebrand, A. Laschewsky, M. Päch, P. Müller-Buschbaum, C. M. Papadakis, *Polym. Chem.* **2017**, 8, 310.
- [112] Y. Fu, L. Zhang, L. Huang, S. Xiao, F. Chen, P. Fan, M. Zhong, J. Yang, *Appl. Surf. Sci.* **2018**, 450, 130.
- [113] S. Peng, H. Wang, W. Zhao, Y. Xin, Yu Liu, X. Yu, M. Zhan, S. Shen, L. Lu, *Adv. Funct. Mater.* **2020**, 30, 2001832.
- [114] X. He, H. Han, L. Liu, W. Shi, X. Lu, J. Dong, W. u Yang, X. Lu, *ACS Appl. Mater. Interfaces* **2019**, 11, 13676.
- [115] A. P. Richez, H. N. Yow, S. Biggs, O. J. Cayre, *Prog. Polym. Sci.* **2012**, 38, 897.
- [116] B. Vincent, *Adv. Colloid Interface Sci.* **1974**, 4, 193.
- [117] T. Tadros, *Adv. Colloid Interface Sci.* **2009**, 147–148, 281.
- [118] B. Ray, B. M. Mandal, *Langmuir* **1997**, 13, 2191.
- [119] M. Vatankhah-Varnoosfaderani, M. Ina, H. Adelnia, Q. Li, A. P. Zhushma, L. J. Hall, S. S. Sheiko, *Macromolecules* **2016**, 49, 7204.
- [120] Z. Huang, S. Nazifi, P. Jafari, A. Karim, H. Ghasemi, *ACS Appl. Bio Mater.* **2020**, 3, 911.
- [121] M. Fan, F. Wang, C. Wang, *Macromol. Biosci.* **2018**, 18, 1800077.
- [122] G. L. Li, H. Möhwald, D. G. Shchukin, *Chem. Soc. Rev.* **2013**, 42, 3628.
- [123] Y. Men, S. Peng, P. Yang, Q. Jiang, Y. Zhang, B. Shen, P. Dong, Z. Pang, W. Yang, *ACS Appl. Mater. Interfaces* **2018**, 10, 23509.
- [124] S. Peng, Y. Men, R. Xie, Y. Tian, W. Yang, *J. Colloid Interface Sci.* **2019**, 539, 19.
- [125] Y. Tian, M. Lei, L. Yan, F. An, *Polym. Chem.* **2020**, 11, 2360.
- [126] M. Chan, A. Almutairi, *Mater. Horiz.* **2016**, 3, 21.
- [127] M. A. Mohsin, N. F. Attia, *Int. J. Polym. Sci.* **2015**, 2015, 436583.
- [128] J. P. Baker, H. W. Blanch, J. M. Prausnitz, *Polymer* **1995**, 36, 1061.
- [129] I. Capek, *Adv. Colloid Interface Sci.* **2010**, 156, 35.
- [130] I. Capek, *Des. Monomers Polym.* **2003**, 6, 399.
- [131] G. Cheng, L. Mi, Z. Cao, H. Xue, Q. Yu, L. Carr, S. Jiang, *Langmuir* **2010**, 26, 6883.
- [132] M. Ajmal, S. Demirci, M. Siddiq, N. Aktas, N. Sahiner, *Colloids Surf., A* **2015**, 486, 29.
- [133] R. Schroeder, W. Richtering, I. I. Potemkin, A. Pich, *Macromolecules* **2018**, 51, 6707.
- [134] T. Nakamura, F. Sugihara, H. Matsushita, Y. Yoshioka, S. Mizukami, K. Kikuchi, *Chem. Sci.* **2015**, 6, 1986.
- [135] X. Li, L. Xing, K. Zheng, P. Wei, L. Du, M. Shen, X. Shi, *ACS Appl. Mater. Interfaces* **2017**, 9, 5817.
- [136] X. Li, Z. Xiong, X. Xu, Y. u Luo, C. Peng, M. Shen, X. Shi, *ACS Appl. Mater. Interfaces* **2016**, 8, 19883.
- [137] W. Li, Q. Liu, P. Zhang, L. Liu, *Acta Biomater.* **2016**, 40, 254.
- [138] P. Saha, M. Santi, M. Frenken, A. R. Palanisamy, R. Ganguly, N. K. Singha, A. Pich, *ACS Macro Lett.* **2020**, 9, 895.
- [139] P. Saha, A. R. Palanisamy, R. Ganguly, S. Mondal, N. K. Singha, M. Santi, A. Pich, *Polym. Adv. Technol.* **2021**, <https://doi.org/10.1002/pat.5214>.
- [140] Z. Zhang, S. Chen, S. Jiang, *Biomacromolecules* **2006**, 7, 3311.
- [141] J. Ladd, Z. Zhang, S. Chen, J. C. Hower, S. Jiang, *Biomacromolecules* **2008**, 9, 1357.
- [142] L. Zheng, H. S. Sundaram, Z. Wei, C. Li, Z. Yuan, *React. Funct. Polym.* **2017**, 118, 51.
- [143] X. Chen, D. Yang, *Biomater. Sci.* **2020**, 8, 4906.
- [144] Á. A. Beltrán-Osuna, J. Ródenas-Rochina, J. L. Gómez Ribelles, J. E. Perilla, *Polym. Adv. Technol.* **2019**, 30, 688.
- [145] J. Zhai, B. Zhou, Y. An, B. Lu, Y. Fan, J. Li, *J. Nanomater.* **2020**, 2020, 7863709.
- [146] J. Oberdisse, T. Hellweg, *Colloid Polym. Sci.* **2020**, 298, 921.
- [147] N. Kihara, Y. Adachi, K. Nakao, T. Fukutomi, *J. Appl. Polym. Sci.* **1998**, 69, 1863.
- [148] W. Shen, Y. Chang, G. Liu, H. Wang, A. Cao, Z. An, *Macromolecules* **2011**, 44, 2524.
- [149] R. Rajan, K. Matsumura, *J. Mater. Chem. B* **2015**, 3, 5683.
- [150] R. Rajan, K. Matsumura, *Sci. Rep.* **2017**, 7, 45777.
- [151] Y. Lu, A. A. Aimetti, R. Langer, Z. Gu, *Nat. Rev. Mater.* **2017**, 2, 16075.
- [152] O. C. Farokhzad, J. Cheng, B. A. Teply, I. Sherif, S. Jon, P. W. Kantoff, J. P. Richie, R. Langer, *Proc. Natl. Acad. Sci. USA* **2006**, 103, 6315.
- [153] N. Ma, Y. Li, H. Xu, Z. Wang, X. i Zhang, *J. Am. Chem. Soc.* **2010**, 132, 442.
- [154] J. Xia, T. Li, C. Lu, H. Xu, *Macromolecules* **2018**, 51, 7435.
- [155] C. Wei, Y. Zhang, H. Xu, Y. Xu, Y. Xu, M. Lang, *J. Mater. Chem. B* **2016**, 4, 5059.
- [156] E. T. M. Dams, P. Laverman, W. J. G. Oyen, G. Storm, G. L. Scherphof, J. W. van Der Meer, F. H. M. Corstens, O. C. Boerman, *J. Pharmacol. Exp. Ther.* **2000**, 292, 1071.
- [157] W. Yang, S. Liu, T. Bai, A. J. Keefe, L. Zhang, J. R. Ella-Menye, Y. Li, S. Jiang, *Nano Today* **2014**, 9, 10.
- [158] S. Peng, B. Ouyang, Y. Xin, W. Zhao, S. Shen, M. Zhan, L. Lu, *Acta Pharm. Sin. B.* **2020**, 11, 560.
- [159] Q. Liu, A. Singh, L. Liu, *Biomacromolecules* **2013**, 14, 226.
- [160] Q. Liu, W. Li, A. Singh, G. Cheng, L. Liu, *Acta Biomater.* **2014**, 10, 2956.
- [161] A. C. Daly, L. Riley, T. Segura, J. A. Burdick, *Nat. Rev. Mater.* **2020**, 5, 20.
- [162] N. Zoratto, D. Di Lisa, J. Rutte, M. d N. Sakib, A. R. Alves E Silva, A. Tamayol, D. Di Carlo, A. Khademhosseini, A. Sheikhi, *Bioeng. Transl. Med.* **2020**, 5, e10180.
- [163] A. Zheng, D. i Wu, M. Fan, H. Wang, Y. Liao, Q. Wang, Y. Yang, *J. Mater. Chem. B* **2020**, 8, 10637.
- [164] E. Sánchez-López, D. Gomes, G. Esteruelas, L. Bonilla, A. L. Lopez-Machado, R. Galindo, A. Cano, M. Espina, M. Ettchetto, A. Camins, A. M. Silva, A. Durazzo, A. Santini, M. L. Garcia, E. B. Souto, *Nanomaterials* **2020**, 10, 292.
- [165] A. Ghavaminejad, C. H. Park, C. S. Kim, *Biomacromolecules* **2016**, 17, 1213.
- [166] Y. Chi, Q. Yuan, Y. Li, J. Tu, L. Zhao, N. Li, X. Li, *J. Colloid Interface Sci.* **2012**, 383, 96.
- [167] P. Saha, M. Santi, M. Emondts, H. Roth, K. Rahimi, J. Großkurth, R. Ganguly, M. Wessling, N. K. Singha, A. Pich, *ACS Appl. Mater. Interfaces* **2020**, 12, 58223.
- [168] X. Yu, J. Liu, Y. Xin, M. Zhan, J. Xiao, L. Lu, S. Peng, *Polym. Chem.* **2019**, 10, 6423.
- [169] S. L. Banerjee, P. Saha, R. Ganguly, K. Bhattacharya, U. Kalita, A. Pich, N. K. Singha, *J. Colloid Interface Sci.* **2021**, 589, 110.
- [170] H. Makki, H. Yahyaei, M. Mohseni, in *Superhydrophobic Polymer Coatings: Fundamentals, Design, Fabrication, and Applications* (Eds: S. K. Samal, S. Mohanty, S. K. Nayak), Elsevier, **2019**.
- [171] T. Li, P. F. Ibáñez-Ibáñez, V. Håkonsen, J. Wu, K. e Xu, Y. Zhuo, S. Luo, J. He, Z. Zhang, *ACS Appl. Mater. Interfaces* **2020**, 12, 35572.
- [172] M. Vatankhah-Varnoosfaderani, X. Hu, Q. Li, H. Adelnia, M. Ina, S. S. Sheiko, *ACS Appl. Mater. Interfaces* **2018**, 10, 20869.
- [173] D. Lu, T. Zhang, J. Ma, *Environ. Sci. Technol.* **2015**, 49, 4235.
- [174] A. K. Kota, G. Kwon, W. Choi, J. M. Mabry, A. Tuteja, *Nat. Commun.* **2012**, 3, 1025.
- [175] J. Rubio, M. L. Souza, R. W. Smith, *Miner. Eng.* **2002**, 15, 139.
- [176] A. L. Ahmad, M. A. Majid, B. S. Ooi, *Desalination* **2011**, 268, 266.

- [177] L. Zang, S. Zheng, L. Wang, J. Ma, L. Sun, *J. Membr. Sci.* **2020**, *612*, 118379.
- [178] X. Li, Z. Ouyang, H. Li, C. Hu, P. Saha, L. Xing, X. Shi, A. Pich, *Bioact. Mater.* **2021**, *6*, 3244.
- [179] X. Li, H. Sun, H. Li, C. Hu, Y. Luo, X. Shi, A. Pich, *Adv. Funct. Mater.* **2021**, <https://doi.org/10.1002/adfm.202100227>.
- [180] L. D. Blackman, P. A. Gunatillake, P. Cass, K. E. S. Locock, *Chem. Soc. Rev.* **2019**, *48*, 757.



Pabitra Saha is currently pursuing his Ph.D. degree at the DWI-Leibniz Institute for Interactive Materials at the RWTH Aachen University under the supervision of Prof. Andrij Pich. He received his B.Sc. degree from the University of Calcutta in 2013. Later on, he obtained his M.Sc. and M.Tech. degrees from the University of Calcutta and Indian Institute of Technology, Kharagpur in 2015 and 2017, respectively. His research areas of interest are zwitterionic functional polymer and block copolymer synthesis and also the development of stimuli-responsive zwitterionic microgels for antifouling coating application.



Ritabrata Ganguly is a graduate student pursuing Ph.D. at the Indian Institute of Technology, Kharagpur under the joint supervision of Prof. Nikhil K. Singha and Prof. Andrij Pich. He received his B.Sc. and B.Tech. degrees from the University of Calcutta Since November 2020, he has been working at the DWI-Leibniz Institute for Interactive Materials, RWTH Aachen University as a visiting research scholar under the DAAD Cotutelle program. His areas of research interest include synthesis of microgels based on functional polymers and block copolymers and study of their solution behavior.



Xin Li received his B.Sc. degree in 2014 from Zhejiang A&F University and M.Sc. degree in 2017 from Donghua University. He is currently working as a Ph.D. candidate in the group of Prof. Andrij Pich in DWI-Leibniz Institute for Interactive Materials at the RWTH Aachen University. His research interests are focused on the development of intelligent hybrid nanoplatforms, including dendrimers, nano/micro/hydrogels, and inorganic nanoparticles for biomedical applications.



Rohas Das is currently pursuing his Ph.D. degree at the Luxembourg Institute of Science and Technology at the University of Luxembourg. He completed his B.Sc. in chemistry (honors) from the University of Calcutta in 2013. Further, he obtained his M.Sc. and M.Tech. degrees from the University of Calcutta and Indian Institute of Technology, Kharagpur in 2015 and 2017, respectively. His research interests are synthesis of functional polymers for application in high strength composites and also development of water-based acrylic pressure sensitive adhesives.



Nikhil K. Singha obtained his Ph.D. from the Indian Institute of Technology, Bombay in 1996. He spent about 7 years researching DSM Research, The Netherlands, in the Dutch Polymer Institute, Eindhoven University of Technology, and in TNO Industries, The Netherlands. He joined the Indian Institute of Technology, Kharagpur in 2003. Presently he is a full professor there. His research interests include the synthesis of functional polymers; block, graft, and star copolymers based on polyacrylates; polyzwitterions; glycopolymers; polyurethanes; and fluoropolymers via RDRP and “click” chemistry and their applications in self-healing, superhydrophobic, shape-memory, thermoplastic elastomers, anti-fouling materials, and their bio-applications.



Andrij Pich obtained his Ph.D. at the Technical University Dresden and Institute of Macromolecular Chemistry and Textile Chemistry in 2001. Afterward, he was a postdoc at the University of Toronto and completed his Habilitation at the Technical University, Dresden in 2008. He was appointed as a professor for Functional and Interactive Polymers at RWTH Aachen University in 2009. In 2019, he was appointed as a part-time professor for Functional Biobased Polymers at Maastricht University. He received the Georg–Manecke–Award of the German Chemical Society (GDCh) in 2007. In 2009, he received a Lichtenberg–Professorship–Grant funded by the VolkswagenStiftung.